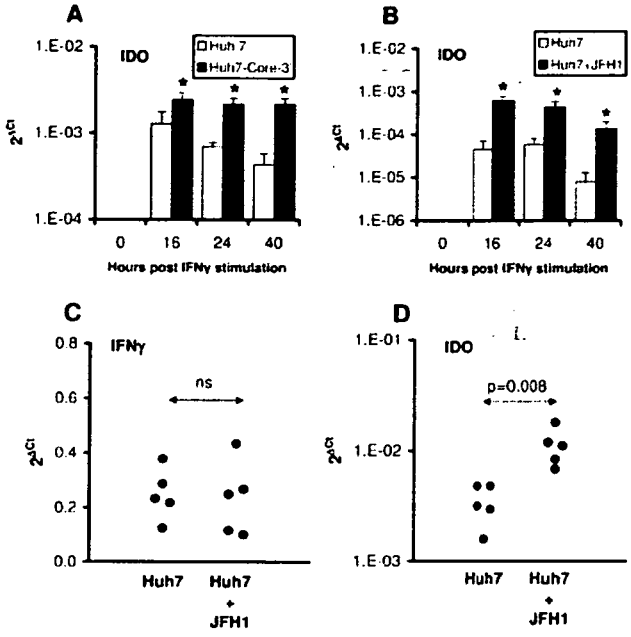

FIG. 2. Induction of IDO mRNA expression by HCV replication. Quantitation of IDO mRNA levels by real-time PCR in Huh7 cells with or without HCV replicon (Huh7-Core-3') (A) or JFH1 virus (B), treated with 100 U/ml of IFN-γ for 0, 16, 24, or 40 h. Results are expressed as the mean ± standard deviations of one representative experiment out of three experiments performed in sextuplicate. (C and D) IDO and IFN-γ mRNA levels measured by real-time PCR in $CD4^+$ $CD25^-$ cells cocultured for 1 day with Huh7 cells with or without HCV-JFH1 in the presence of Dynabeads CD3/CD28 T-cell expander. All results are normalized with β-actin. Statistical analyses were performed using the nonparametric Mann-Whitney U test. (*, $P < 0.01$; Huh7-core 3' versus Huh7 or Huh7 plus JFH1 versus Huh7). ns, not significant.

resist immune attack is by promoting IDO expression when infected hepatocytes interact with effector T cells producing IFN-γ. To test this hypothesis, Huh7 cells infected with JFH1 and control Huh7 cells were cocultured with 1.2×10^5 $CD4^+$ $CD25^-$ cells from a healthy subject (using the negative fraction of the CD4+CD25+ Regulatory T Cell Isolation kit; Miltenyi Biotec, Bergisch Gladbach, Germany) in the presence of the Dynabeads CD3/CD28 T-cell expander (Dynal biotech, Oslo, Norway) to activate T cells. After 1 day, the coculture was collected and both IFN-γ mRNA and IDO mRNA were determined by quantitative real-time PCR (IFN-γ sense primer, CTCTGCATCGTTTTGGGTTC; antisense, GCGTTGGAC ATTCAAGTCAG). As shown in Fig. 2C and D, the induction of IFN-γ was similar in cocultures containing control and infected Huh7 cells, but the expression of IDO was significantly higher in HCV-infected cultures. Since IDO levels were about 100-fold higher in coculture experiments than in experiments using exogenous IFN-γ, whether other factors apart from IFN-γ, such as cell contact, might be involved in this high IDO upregulation was studied. Thus, when supernatant from activated $CD4^+$ $CD25^-$ T cells was added to infected or noninfected Huh7 cells, differences in IDO upregulation were not observed (data not shown). It appears, therefore, that IDO induction is mainly facilitated by cell contact between infected cells and activated T lymphocytes. Whether IDO induction in livers with CHC takes place in infected hepatocytes and/or in inflammatory mononuclear cells has not been analyzed in the present work. However, our data for HCV-infected hepatoma cells suggest that hepatocytes are at least partially responsible for the elevated hepatic levels of IDO found in CHC.

There is an intricate cross talk between IDO and CTLA-4 (17). It has been shown that tryptophan depletion together with the presence of kynurenines promotes the expression of inhibitory molecules, such as CTLA-4 and Foxp3, in T cells (5). On the other hand, CTLA-4 stimulates IDO expression and IDO activity in antigen-presenting cells, inducing tolerogenic dendritic cells (17). Thus, we investigated whether IDO expression in the liver might correlate with the abundance of CTLA-4 mRNA in this organ. By using quantitative real-time PCR (CTLA-4 sense primer, TCATGTACCCACCGCCATAC; antisense, TAGACCCCTGTTGTAAGAGG), we found that CTLA-4 mRNA levels were increased in liver biopsy samples from HCV-infected patients over those in normal hepatic tissue or in samples from patients with SVR or other forms of liver disease (Fig. 3A). A significant direct correlation was found between IDO mRNA levels and CTLA-4 mRNA levels in liver tissue from HCV-infected patients ($r = 0.52$; $P < 0.01$) (Fig. 3B).

Liver biopsies are not routinely performed for patients with acute hepatitis C. Thus, in order to investigate the role of hepatic IDO expression in the evolution of HCV infection, we analyzed serial liver biopsy samples obtained from six chimpanzees after they were infected with 25 50% chimpanzee infectious doses of the HCV 1b J4 virus stock (Robert H. Purcell, NIAID, NIH, Bethesda, MD). This study was approved by independent ethical committees in accordance with international regulations (International Animal Care and Use Committee). As shown in Fig. 3C, hepatic IDO mRNA declined after an initial peak and remained low during evolution in animals that cleared the virus, while in the chimpanzees that evolved to chronicity, the initial peak of IDO expression was lower but the levels remained elevated during evolution. Thus, both in chimpanzees and in humans, chronic HCV infection is associated with persistently high IDO expression in the liver. An initial short-lived upregulation of IDO in the animals that cleared the virus might be secondary to the induction of a potent and efficient immune response. In fact, an early and transient upsurge of IDO might take place in association with activation of dendritic cells and T-cell immunity (11), while persistent IDO overexpression may favor tolerance (17). Our findings for acute infection in chimpanzees lend support to this contention.

In parallel to IDO results, for chimps that cured the infection, CTLA-4 expression in the liver showed an initial peak and then remained stable at very low levels during the evolution of the disease (Fig. 3D). In contrast, for chimps that became chronic carriers, expression of CTLA-4 showed little change during the early phase of infection but tended to persist above basal values along the course of the infection (Fig. 3D). As with humans, we found a significant direct correlation between IDO and CTLA-4 mRNA values in the liver (Fig. 3E).

In summary, we show upregulation of IDO in the livers of patients and chimpanzees with chronic hepatitis C. This finding is associated, and correlates, with overexpression of CTLA-4 in liver tissue. Our data indicate that HCV infection facilitates

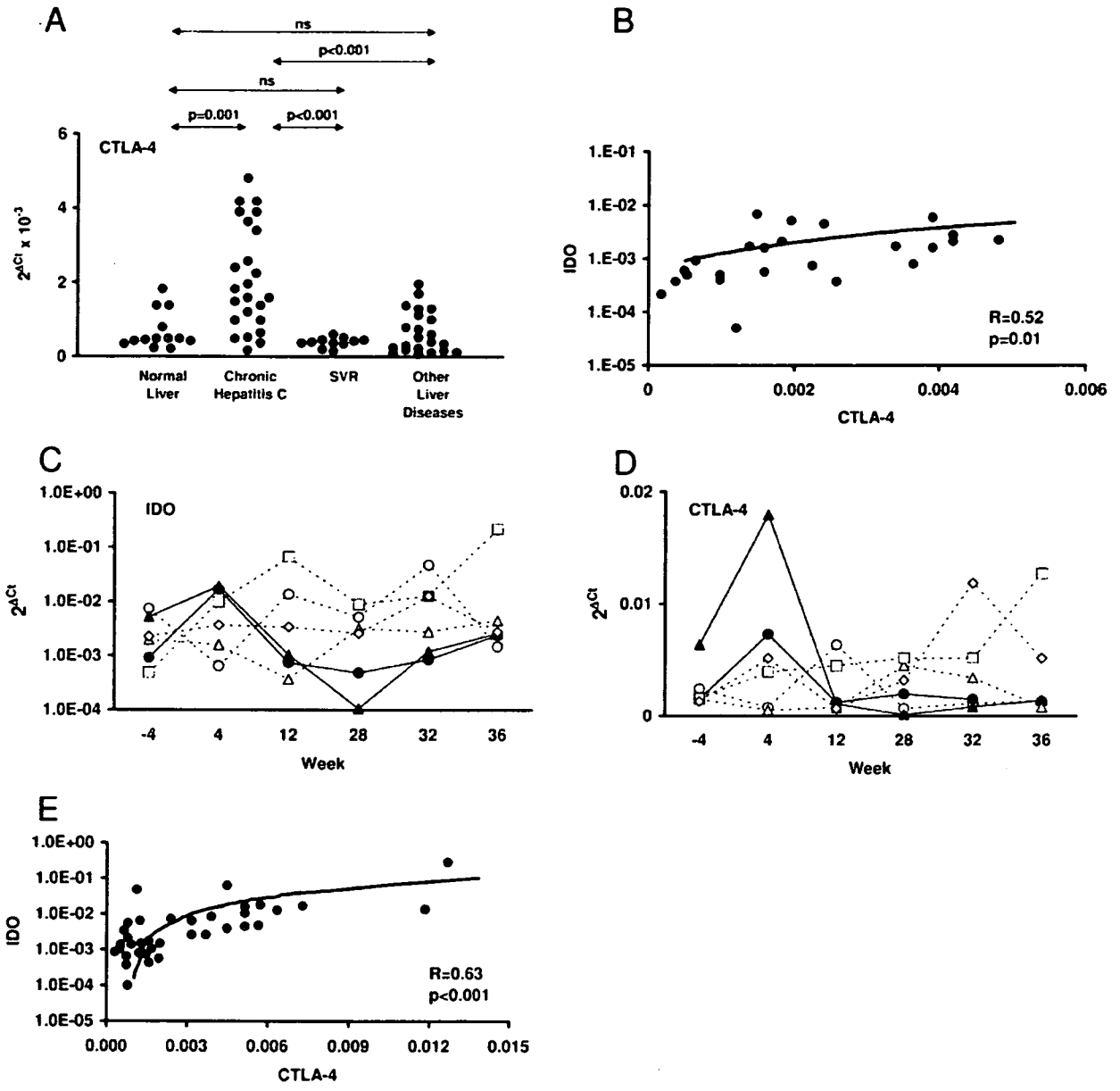

FIG. 3. CTLA-4 and HCV infection. (A) Real-time PCR quantitation of CTLA-4 mRNA in samples from normal livers or from livers from patients with CHC, from patients with CHC who cleared the virus after interferon therapy (SVR), or from a miscellaneous group of patients with liver disorders unrelated to HCV. Statistical analyses were performed using nonparametric Kruskal-Wallis and Mann-Whitney U tests. ns, not significant. (B) Correlation between mRNA levels of IDO and CTLA-4 in liver samples from CHC patients. (C and D) Real-time PCR quantitation of IDO and CTLA-4 mRNA levels in liver samples from chimpanzees obtained at different time points before and after infection with infective HCV inocula, with 0 being the week of infection. Solid lines, chimpanzees who cleared HCV infection; dotted lines, chimpanzees who did not clear HCV infection. (E) Correlation between mRNA levels of IDO and CTLA-4 in liver samples from the chimpanzees described above. Results in panels A, C, and D are normalized with β-actin.

the induction of IDO in response to proinflammatory cytokines and activated T cells. This may constitute an efficient strategy of the virus to escape T-cell immunity. Our findings point to novel targets for therapeutic intervention.

We thank E. Elizalde, S. Jusué, M. Corres, V. Villar, and M. Gorraiz for their technical support and R. Bartenschlager for kindly providing the HCV replicon.

This work was supported by grants from Instituto de Salud Carlos III, Ref PI060149, PI051098, and 03/0566, from Ministerio de Educación y Ciencia (SAF2004-01680), from Fundación de Investigación Médica Mutua Madrileña, and from the European Union (QLK2-CT-1999-00356). T. Wakita is supported by a grant-in-aid for Scientific Research from the Japan Society for the Promotion of Science, from the Ministry of Health, Labor and Welfare of Japan, and from the Ministry of Education, Culture, Sports, Science and Technology. This project was also funded by "UTE project CIMA."

REFERENCES

1. **Abbate, I., M. Romano, R. Longo, G. Cappiello, O. Lo Iacono, V. Di Marco, C. Paparella, A. Spano, and M. R. Capobianchi.** 2003. Endogenous levels of mRNA for IFNs and IFN-related genes in hepatic biopsies of chronic HCV-infected and non-alcoholic steatohepatitis patients. J. Med. Virol. **70**:581–587.
2. **Botarelli, P., M. R. Brunetto, M. A. Minutello, P. Calvo, D. Unutmaz, A. J. Weiner, Q. L. Choo, J. R. Shuster, G. Kuo, F. Bonino, M. Houghton, and S. Abrignani.** 1993. T-lymphocyte response to hepatitis C virus in different clinical courses of infection. Gastroenterology **104**:580–587.
3. **Diepolder, H. M., R. Zachoval, R. M. Hoffmann, E. A. Wierenga, T. Santantonio, M. C. Jung, D. Eichenlaub, and G. R. Pape.** 1995. Possible mechanism involving T-lymphocyte response to non-structural protein 3 in viral clearance in acute hepatitis C virus infection. Lancet **346**:1006–1007.
4. **Fallarino, F., U. Grohmann, K. W. Hwang, C. Orabona, C. Vacca, R. Bianchi, M. L. Belladonna, M. C. Fioretti, M. L. Alegre, and P. Puccetti.** 2003. Modulation of tryptophan catabolism by regulatory T cells. Nat. Immunol. **4**:1206–1212.
5. **Fallarino, F., U. Grohmann, S. You, B. C. McGrath, D. R. Cavener, C. Vacca, C. Orabona, R. Bianchi, M. L. Belladonna, C. Volpi, P. Santamaria, M. C. Fioretti, and P. Puccetti.** 2006. The combined effects of tryptophan starvation and tryptophan catabolites down-regulate T cell receptor zeta-chain and induce a regulatory phenotype in naive T cells. J. Immunol. **176**:6752–6761.
6. **Ferrari, C., A. Valli, L. Galati, A. Penna, P. Scaccaglia, T. Giuberti, C. Schianchi, G. Missale, M. G. Marin, and F. Fiaccadori.** 1994. T-cell response to structural and nonstructural hepatitis C virus antigens in persistent and self-limited hepatitis C virus infections. Hepatology **19**:286–295.
7. **Frumento, G., R. Rotondo, M. Tonetti, G. Damonte, U. Benatti, and G. B. Ferrara.** 2002. Tryptophan-derived catabolites are responsible for inhibition of T and natural killer cell proliferation induced by indoleamine 2,3-dioxygenase. J. Exp. Med. **196**:459–468.
8. **Grohmann, U., F. Fallarino, R. Bianchi, C. Orabona, C. Vacca, M. C. Fioretti, and P. Puccetti.** 2003. A defect in tryptophan catabolism impairs tolerance in nonobese diabetic mice. J. Exp. Med. **198**:153–160.
9. **Grohmann, U., C. Orabona, F. Fallarino, C. Vacca, F. Calcinaro, A. Falorni, P. Candeloro, M. L. Belladonna, R. Bianchi, M. C. Fioretti, and P. Puccetti.** 2002. CTLA-4-Ig regulates tryptophan catabolism in vivo. Nat. Immunol. **3**:1097–1101.
10. **Hoffmann, R. M., H. M. Diepolder, R. Zachoval, F. M. Zwiebel, M. C. Jung, S. Scholz, H. Nitschko, G. Riethmuller, and G. R. Pape.** 1995. Mapping of immunodominant CD4+ T lymphocyte epitopes of hepatitis C virus antigens and their relevance during the course of chronic infection. Hepatology **21**: 632–638.
11. **Hwang, S. L., N. P. Chung, J. K. Chan, and C. L. Lin.** 2005. Indoleamine 2,3-dioxygenase (IDO) is essential for dendritic cell activation and chemotactic responsiveness to chemokines. Cell Res. **15**:167–175.
12. **Larrea, E., R. Aldabe, E. Molano, C. M. Fernandez-Rodriguez, A. Ametzazurra, M. P. Civeira, and J. Prieto.** 2006. Altered expression and activation of STATs (signal transduction and activator of transcription) in HCV infection: in vivo and in vitro studies. Gut **55**:1179–1187.
13. **Larrea, E., R. Aldabe, J. I. Riezu-Boj, A. Guitart, M. P. Civeira, J. Prieto, and E. Baixeras.** 2004. IFN-alpha5 mediates stronger Tyk2-stat-dependent activation and higher expression of 2′,5′-oligoadenylate synthetase than IFN-alpha2 in liver cells. J. Interferon Cytokine Res. **24**:497–503.
14. **Lasarte, J. J., M. Garcia Granero, A. Lopez, N. Casares, N. Garcia, M. P. Civeira, F. Borras Cuesta, and J. Prieto.** 1998. Cellular immunity to hepatitis C virus core protein and the response to interferon in patients with chronic hepatitis C. Hepatology **28**:815–822.
15. **Lee, G. K., H. J. Park, M. Macleod, P. Chandler, D. H. Munn, and A. L. Mellor.** 2002. Tryptophan deprivation sensitizes activated T cells to apoptosis prior to cell division. Immunology **107**:452–460.
16. **Lohmann, V., F. Korner, J. Koch, U. Herian, L. Theilmann, and R. Bartenschlager.** 1999. Replication of subgenomic hepatitis C virus RNAs in a hepatoma cell line. Science **285**:110–113.
17. **Mellor, A. L., and D. H. Munn.** 2004. IDO expression by dendritic cells: tolerance and tryptophan catabolism. Nat. Rev. Immunol. **4**:762–774.
18. **Missale, G., R. Bertoni, V. Lamonaca, A. Valli, M. Massari, C. Mori, M. G. Rumi, M. Houghton, F. Fiaccadori, and C. Ferrari.** 1996. Different clinical behaviors of acute hepatitis C virus infection are associated with different vigor of the anti-viral cell-mediated immune response. J. Clin. Investig. **98**:706–714.
19. **Miwa, N., S. Hayakawa, S. Miyazaki, S. Myojo, Y. Sasaki, M. Sakai, O. Takikawa, and S. Saito.** 2005. IDO expression on decidual and peripheral blood dendritic cells and monocytes/macrophages after treatment with CTLA-4 or interferon-γ increase in normal pregnancy but decrease in spontaneous abortion. Mol. Hum. Reprod. **11**:865–870.
20. **Munn, D. H.** 2006. Indoleamine 2,3-dioxygenase, tumor-induced tolerance and counter-regulation. Curr. Opin. Immunol. **18**:220–225.
21. **Munn, D. H., M. Zhou, J. T. Attwood, I. Bondarev, S. J. Conway, B. Marshall, C. Brown, and A. L. Mellor.** 1998. Prevention of allogeneic fetal rejection by tryptophan catabolism. Science **281**:1191–1193.
22. **Platten, M., P. P. Ho, S. Youssef, P. Fontoura, H. Garren, E. M. Hur, R. Gupta, L. Y. Lee, B. A. Kidd, W. H. Robinson, R. A. Sobel, M. L. Selley, and L. Steinman.** 2005. Treatment of autoimmune neuroinflammation with a synthetic tryptophan metabolite. Science **310**:850–855.
23. **Rehermann, B., K. M. Chang, J. G. McHutchison, R. Kokka, M. Houghton, and F. V. Chisari.** 1996. Quantitative analysis of the peripheral blood cytotoxic T lymphocyte response in patients with chronic hepatitis C virus infection. J. Clin. Investig. **98**:1432–1440.
24. **Sarobe, P., J. I. Jauregui, J. J. Lasarte, N. Garcia, M. P. Civeira, F. Borras-Cuesta, and J. Prieto.** 1996. Production of interleukin-2 in response to synthetic peptides from hepatitis C virus E1 protein in patients with chronic hepatitis C: relationship with the response to interferon treatment. J. Hepatol. **25**:1–9.
25. **Taylor, M. W., and G. S. Feng.** 1991. Relationship between interferon-gamma, indoleamine 2,3-dioxygenase, and tryptophan catabolism. FASEB J. **5**:2516–2522.
26. **Terness, P., T. M. Bauer, L. Rose, C. Dufter, A. Watzlik, H. Simon, and G. Opelz.** 2002. Inhibition of allogeneic T cell proliferation by indoleamine 2,3-dioxygenase-expressing dendritic cells: mediation of suppression by tryptophan metabolites. J. Exp. Med. **196**:447–457.
27. **Widner, B., E. R. Werner, H. Schennach, H. Wachter, and D. Fuchs.** 1997. Simultaneous measurement of serum tryptophan and kynurenine by HPLC. Clin. Chem. **43**:2424–2426.
28. **Zhong, J., P. Gastaminza, G. Cheng, S. Kapadia, T. Kato, D. R. Burton, S. F. Wieland, S. L. Uprichard, T. Wakita, and F. V. Chisari.** 2005. Robust hepatitis C virus infection in vitro. Proc. Natl. Acad. Sci. USA **102**:9294–9299.

Hepatology Research 2007; 37: 433–443 doi: 10.1111/j.1872-034X.2007.00056.x

Original Article

An infectious and selectable full-length replicon system with hepatitis C virus JFH-1 strain

Tomoko Date,[1]* Michiko Miyamoto,[1] Takanobu Kato,[2,3] Kenichi Morikawa,[1]* Asako Murayama,[1]* Daisuke Akazawa,[1,4]* Junichi Tanabe,[1,4] Saburo Sone,[4] Masashi Mizokami[2] and Takaji Wakita[1]*

[1]*Department of Microbiology, Tokyo Metropolitan Institute for Neuroscience, Tokyo,* [2]*Department of Clinical Molecular Informative Medicine, Nagoya City University Graduate School of Medical Sciences, Nagoya, and* [4]*Pharmaceutical Research Laboratory, Toray Industries Inc., Kanagawa, Japan; and* [3]*Liver Disease Branch, NIDDK, National Institute of Health, Bethesda, Maryland, USA*

Aim: The hepatitis C virus (HCV) strain JFH-1 was cloned from a patient with fulminant hepatitis. A JFH-1 subgenomic replicon and full-length JFH-1 RNA efficiently replicate in cultured cells. In this study, an infectious, selectable HCV replicon containing full-length JFH-1 cDNA was constructed.

Methods: The full-genome replicon was constructed using the neomycin-resistant gene, EMCV IRES and wild-type JFH-1 cDNA. Huh7 cells were transfected with RNA synthesized *in vitro*, and then cultured with G418. Independent colonies were cloned to establish cell lines that replicate the full-length HCV replicon.

Results: HCV RNA replication was detected in each isolated cell line. HCV proteins and HCV RNA were secreted into culture medium, and exhibited identical density profiles. Interestingly, culture supernatants of the replicon cells were infectious for naïve Huh7 cells. Long-term culture did not affect replication of replicon RNA in the replicon cells, but it reduced core protein secretion and infectivity of culture supernatant. Culture supernatant obtained after serial passage of replicon virus was infectious for Huh7 cells.

Conclusions: Selectable infection was established using HCV replicon containing full-length genotype 2a JFH-1 cDNA. This system might be useful for HCV research.

Key words: hepatitis C virus, infectious virus, replicon, RNA replication

INTRODUCTION

HEPATITIS C VIRUS (HCV) is a plus-strand RNA virus and is the principal cause of post-transfusion hepatitis and sporadic acute hepatitis.[1,2] Infection with HCV causes chronic liver diseases, including cirrhosis and hepatocellular carcinoma.[3] Although HCV belongs to the *Flaviviridae* family, and has a genome structure similar to other flaviviruses, it has been difficult to develop an efficient cell culture system for HCV.[4] A subgenomic HCV RNA replicon system has been developed,[5] enabling assessment of HCV replication in cultured cells. Although that system is a powerful tool for studies of HCV replication mechanisms and development of antiviral agents, its replicon cells do not produce infectious viral particles, even when the replicons contain structural genes.[6,7] Studies conducted using the above replicon system indicate that wild-type HCV genomes have low replication capacities.[7,8]

Adaptive mutations can substantially increase replication of HCV, but introduction of these adaptive mutations into full-length genomes causes loss of infectivity *in vivo*.[8] The JFH-1 strain was cloned from a patient with fulminant hepatitis, and its sequence differs from those of chronic hepatitis isolates.[9] Using JFH-1 cDNA, we previously established subgenomic replicon constructs that replicate in Huh7 cells with greater efficiency than other HCV strains, and that also replicate in other cell lines.[10,11] In a previous study, when we transfected Huh7 cells with *in-vitro*-transcribed full-length JFH-1 HCV RNA, the JFH-1 RNA efficiently replicated and the cells produced viral particles that were infectious for cultured cells and a chimpanzee.[12] In the present study, we established a full-length HCV replicon using the JFH-1 strain.

Correspondence: Dr Takaji Wakita, Department of Virology II, National Institute of Infectious Diseases, 1-23-1 Toyama, Shinjuku, Tokyo 162-8640, Japan. Email: wakita@nih.go.jp
*Present address: Department of Virology II, National Institute of Infectious Diseases, Tokyo, Japan.
Received 10 November 2006; revision 4 December 2006; accepted 5 December 2006.

Replicon virus particles were secreted from the replicon cells, and the replicon virus was infectious for naïve Huh7 cells.

METHODS

Cell culture system

HUH7 CELLS WERE donated by Dr Tetsuro Suzuki (National Institute of Infectious Diseases, Tokyo, Japan), and were cultured at 37°C in Dulbecco's modified Eagle's medium containing 10% fetal bovine serum (DMEM-10), as previously described.[10]

Construction of the full-genome HCV replicon

A full-genome replicon construct of JFH-1 (pFGR-JFH1; Fig. 1a) was assembled based on the consensus sequence of JFH-1, as follows. The gene for the encephalomyocarditis virus (EMCV) internal ribosomal entry site (IRES) was amplified from a subgenomic replicon construct of JFH-1 (pSGR-JFH1; Fig. 1a)[10] using the primers Pm/EI-S (5'-AGC TTT GTT TAA ACC CTC TCC CTC CCC CCC CCC TAA CGT T-3'; the underlined segment is the *PmeI* site) and EI/FH/Core-R (5'-TGA GGT TTA GGA TTT GTG CTC ATG GTA TCA TCG TGT TTT T-3'). The core region was amplified from pJFH1[12] using the primers EI/FH/Core-S (5'- TTG AAA AAC ACG ATG ATA CCA TGA GCA CAA ATC CTA AAC C-3') and FH/1592-R (5'- CGG TTG ATG TGC CAA CTG CC-3'). These two polymerase chain reaction (PCR) fragments were purified, mixed and reamplified using the primers Pm/EI-S and FH/1592-R. Reamplified PCR product was digested with *PmeI* and *BsiWI*. Another DNA fragment containing a 5' untranslated region (5' UTR) and neomycin-resistant gene was digested from pSGR-JFH1 using *AgeI* and *PmeI* (Fig. 1a). These two DNA fragments were cloned into the vector pJFH1 at sites for *AgeI* and *BsiWI* to produce the pFGR-JFH1 construct (accession number: AB237837, Fig. 1a).

As a control, we also created the mutant construct pFGR-JFH1/GND that includes a point mutation that changes a GDD motif to GND, which abolishes the RNA polymerase activity of non-structural protein (NS) 5B.[10]

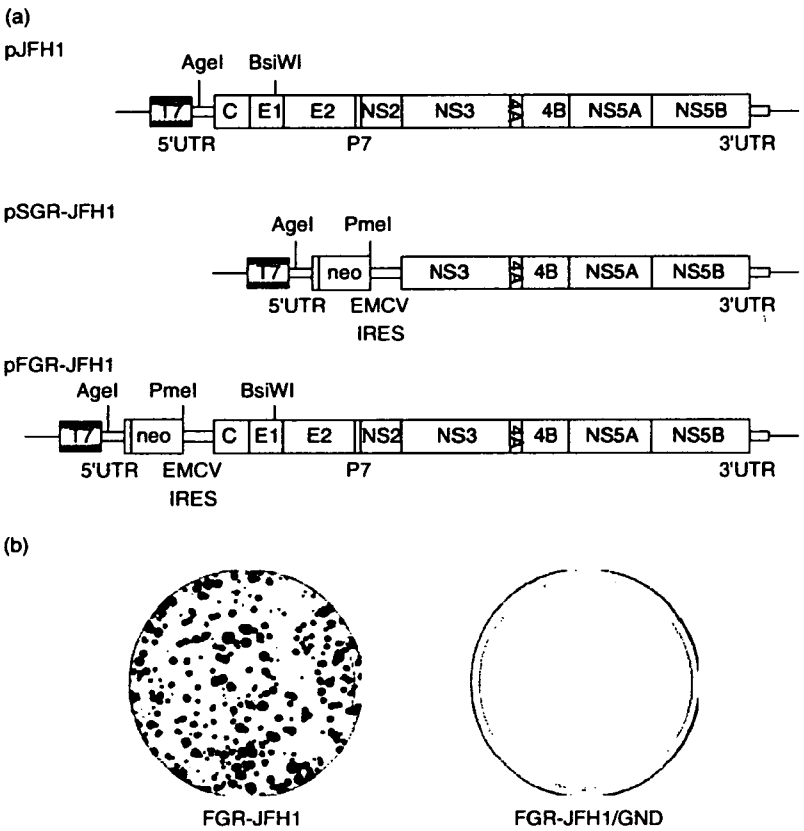

Figure 1 Structure of the full-genome hepatitis C virus (HCV) RNA replicon constructed from genotype 2a JFH-1 and colony formation of replicon RNA-transfected Huh7 cells. (a) Organization of the full-length JFH-1 genome (top), subgenomic replicon construct pSGR-JFH1 (middle) and full-genome replicon construct pFGR-JFH1 (bottom). Open reading frames (thick boxes) are flanked by untranslated regions (thin boxes). '*AgeI*', '*BsiWI*' and '*PmeI*' indicate positions of restriction sites. A T7 RNA promoter is located upstream from the 5' end of the replicon construct. (b) Colony formation of JFH-1 HCV full-genome replicon. Huh7 cells were transfected with transcribed RNA (1 μg), and transfected cells were cultured in medium supplemented with G418 (1 mg/mL) for 3 weeks before staining with crystal violet.

All plasmid DNA was transformed using DH5 α-competent cells. Amplified plasmid DNA was purified by performing ultra-centrifugation twice.

RNA synthesis

Replicon RNA was synthesized as described previously.[10,12] Briefly, the plasmid pFGR-JFH1 was digested with *XbaI* and treated with Mung Bean nuclease (New England Biolabs, Beverly, MA, USA). Digested plasmid DNA fragments were purified and used as templates for RNA synthesis. HCV RNA was synthesized *in vitro* using a MEGAscript T7 kit (Ambion, Austin, TX, USA). Synthesized RNA was treated with DNaseI, followed by acid phenol extraction to remove any remaining template DNA.

RNA transfection and colony formation experiment

Synthesized replicon RNA was used for transfection via electroporation. Synthesized RNA (0.1 ng to 10 μg) was adjusted to 10 μg with cellular RNA isolated from untransfected Huh7 cells. Naïve Huh7 cells were transfected with transcribed replicon RNA from pFGR-JFH1, or were transfected with control RNA transcribed from pFGR-JFH1/GND, in which the catalytic domain of the RNA polymerase NS5B is mutated. Trypsinized Huh7 cells were washed with Opti-MEM I reduced-serum medium (Invitrogen, Carlsbad, CA, USA) and resuspended at 7.5×10^6 cells/mL with Cytomix buffer.[10] RNA (10 μg) was mixed with 400 μL of cell suspension and transferred to an electroporation cuvette (Precision Universal Cuvettes, Thermo Hybrid, Middlesex, UK). The cells were then pulsed at 260 V and 950 μF with the Gene Pulser II apparatus (Bio-Rad, Hercules, CA, USA). Transfected cells were immediately transferred to 10-cm culture dishes, each containing 8 mL of culture medium. G418 (1.0 mg/mL) (Nacalai Tesque, Kyoto, Japan) was added to the culture medium at 16–24 h after transfection. Culture medium supplemented with G418 was replaced twice per week.

Three weeks after transfection, cells were fixed with buffered formalin and stained with crystal violet. Colony formation efficiency of the transfected cells was determined by counting the number of colonies that formed.

Analysis of G418-resistant cells

Sparsely grown G418-resistant colonies were independently isolated using a cloning cylinder (Asahi Techno Glass, Tokyo, Japan), and were expanded until they were 80–90% confluent in 10-cm dishes. Expanded cells were harvested for nucleic acid and protein analyses. Total RNA and genomic DNA were simultaneously isolated from expanded cells using the Isogen reagent (Nippon Gene, Tokyo, Japan). Another portion of each cell pellet was dissolved with radioimmune precipitation assay (RIPA) buffer containing 0.1% SDS. Eight cloned cell lines were selected for further analysis.

Northern blot analysis

Isolated RNA fragments (4 μg) were separated in a 1% agarose gel containing formaldehyde, transferred to a positively charged nylon membrane (Hybond-N+, Amersham Pharmacia, Buckinghamshire, UK), and immobilized by Stratalinker UV crosslinker (Stratagene, La Jolla, CA, USA). Replicon RNA was detected using probes specific for certain positions. Hybridization was performed using a [α-^{32}P]dCTP-labeled DNA probe and Rapid-Hyb buffer (Amersham Pharmacia). The DNA probe was synthesized from the genes *neo*^{r} and EMCV IRES, using the Megaprime DNA labeling system (Amersham Pharmacia).

Western blotting and immunofluorescence analysis

We analyzed protein expression in replicon cells by performing western blotting and immunofluorescence. Cells were lysed using a RIPA buffer containing 0.1% SDS, 0.5% NP-40, 10 mM Tris-HCl (pH 7.4), 1 mM ethylenediaminetetraacetic acid (EDTA), and 150 mM NaCl. Protein samples were separated on 10% or 12% polyacrylamide gels, and were subsequently transferred to a polyvinylidene difluoride membrane (Millipore, Tokyo, Japan). Transferred proteins were incubated with blocking buffer containing 5% non-fat dried milk in phosphate-buffered saline (PBS). HCV proteins were detected using anticore monoclonal antibodies (25, clone 2H9), anti-E1 and anti-E2 polyclonal antibodies,[12] anti-NS3 polyclonal antibodies,[10] anti-NS5A polyclonal antibodies,[11] peroxidase-labeled goat antirabbit IgG (Biosource), and peroxidase-labeled sheep antimouse IgG (Amersham Pharmacia). Signals were detected using a chemiluminescence system (Amersham Pharmacia).

Cells containing the HCV replicon were grown on a cover glass, and were then fixed in acetone-methanol (1:1 v/v) for 10 min at −20°C. Cells were then incubated in immunofluorescence assay buffer (PBS, 1% bovine serum albumin, 2.5 mM EDTA). Anti-core monoclonal antibodies or anti-NS3 and anti-NS5a polyclonal antibodies were added at 50 μg/mL or a dilution of 1:50, respectively, in immunofluorescence buffer. After incubation for 1 h at room temperature, cells were washed,

followed by incubation with fluorescein isothiocyanate-conjugated antimouse IgG (Cappel, Durham, NC, USA) in immunofluorescence assay buffer. Cover slips were washed and mounted on glass slides using Shandon PermaFluor mounting solution (Thermo Electron, Pittsburgh, PA, USA). Cells were examined by fluorescence microscopy (Carl Zeiss, Oberkochen, Germany).

To assay secretion of viral protein and virus particles into culture medium from cells replicating replicon RNA, we measured levels of core protein in culture medium using a sensitive immunoassay. Culture supernatants from all eight replicon cell lines were used in this immunoassay.

Genomic DNA PCR

To detect integration of the *neo*^{r} gene into the genomic DNA, isolated cellular genomic DNA was amplified by PCR using *neo*^{r}-specific primers (NEO-S3; 5′-AACAA GATGGATTGCACGCA-3′, NEO-R; 5′-CGTCAAGAAG GCGATAGAAG-3′).

RT-PCR and sequencing analysis

We sequenced the replicating HCV RNA in each of the eight selected clones. The cDNAs of the HCV RNA replicon were synthesized from total RNA isolated from cells using a reverse primer for the 3′× region. These cDNAs were subsequently amplified with DNA polymerase (TaKaRa LA *Taq*, Takara Bio, Shiga, Japan). Six separate PCR primer sets were used to amplify the following sections of the pFGR-JFH1 replicon construct, to cover the entire open reading frame: nt 151–2043, nt 1913–3778, nt 3597–6046, nt 5997–8685, nt 8649–10782, and nt 10713–11017. The sequence of each amplified DNA was determined.

Quantification of HCV core protein and RNA

To estimate levels of HCV core protein in culture supernatant, concentrations of HCV core protein were measured. Aliquots (250 μL) of samples were assayed using a new immunoassay technique described elsewhere.[13] Total RNA was isolated from harvested cells or culture media using Isogen. Copy numbers of HCV RNA were determined by real-time detection reverse transcription (RT)-PCR, using an ABI Prism 7700 sequence detector system (Applied Biosystems, Tokyo, Japan).[14]

Density gradient analysis

To determine whether secreted viral core protein was incorporated in viral particles, we analyzed culture medium by sucrose density gradient centrifugation. Culture medium derived from replicon cells was harvested for density gradient analysis. Collected culture medium was cleared by low-speed centrifugation at 2000 r.p.m. for 10 min, and was then passed through a disk filter with a pore size of 0.45 μm (Millipore). Filtered culture medium was layered on a stepwise sucrose gradient (60% to 10%, wt/vol) and centrifuged for 16 h in a SW41 rotor (Beckman, Palo Alto, CA, USA) at 40 000 r.p.m. at 4°C. After centrifugation, 22 fractions were harvested from the bottoms of the tubes. The core protein concentration of each fraction was measured by performing an immunoassay using 100 μL of the fraction. The HCV RNA titer of each fraction was determined by real time detection RT-PCR using RNA isolated from 100 μL of the fraction.

Infectivity of secreted viral particles

To assess the infectivity of secreted viral particles, naïve Huh7 cells were inoculated with culture supernatant from replicon cell lines. Culture supernatant used for inoculation was centrifuged and filtered to remove cell debris. Cleared culture supernatant was concentrated by ultrafiltration as described previously,[12] and G418 was removed from the concentrated culture supernatant during ultrafiltration. Naïve Huh7 cells were inoculated with concentrated culture medium. Inoculated cells were cultured for 3 weeks in medium supplemented with G418 (0.3 mg/mL).

Long-term culture of replicon cells

To examine replicon RNA replication and virus secretion and infectivity after long-term culture, the eight replicon clones were serially passaged for more than 7 months. HCV RNA levels in replicon cells were measured by real time detection RT-PCR. Infectivity of culture supernatants was determined by measuring colony formation efficiency.

Serial passage of replicon virus

To examine long-term replicon virus passage, replicon virus was serially passaged for approximately 6 months. Culture supernatants harvested from the replicon-RNA-transfected Huh7 cells were used to inoculate naïve Huh7 cells. Inoculated cells formed colonies after 4 weeks of G418 selection culture. This infection and selection procedure was repeated seven times. Infectivity of culture supernatants was determined by measuring colony formation.

Statistical analysis

Statistical analysis was performed using the Mann–Whitney *U*-test or Student's *t*-test. *P*-values of <0.05 were considered to indicate significance.

RESULTS

Construction of full-genome replicon using JFH-1, and colony formation

FIGURE 1A SHOWS the full-genome replicon construct pFGR-JFH1, which was produced from the full-length JFH-1 construct pJFH1 and which contains a neomycin-resistant gene.[12] Huh7 cells transfected with pFGR-JFH1 replicon RNA formed colonies efficiently (Fig. 1b). Huh7 cells transfected with control RNA transcribed from pFGR-JFH1/GND did not form colonies. Cells transfected with full-genome replicon RNA formed colonies 80.7-fold less efficiently than cells transfected with JFH-1 subgenomic replicon RNA (Table 1).[10]

Analysis of replicon cells

Figure 2a shows the results of northern blot analysis of replicon RNA replication in the cloned cell lines using cellular RNA extracted from each replicon cell. Intensities of replicon RNA signals differed among the eight clones. Replicon RNAs were clearly identified at the same position as in control RNA; however, additional specific signals were present higher on the gel as was also observed in subgenomic replicon cells.[10] These signals may represent replication intermediates or double-stranded RNA. The replicon RNA titer ranged from 1.14×10^7 to 7.09×10^7 copies/μg cellular RNA (Table 2). We also estimated the replicon RNA copy numbers per cell. Full-genome replicon cell clones were harvested and counted 2 days after passage. Mean HCV RNA titer of eight full-genomic replicon clones was 6.93×10^3 copy/cell. RNA replication levels in the full-genomic replicon cells were at the similar level with subgenomic JFH-1 replicon cells.[10]

Figure 2b shows the results of western blot analysis. In the cell lysate extracted from each replicon cell, we detected core, E1, E2, NS3 and NS5a proteins at the expected positions. Signals detected by anti-NS5a antibody exhibited doublet bands that may represent p58 and p56 with different degrees of phosphorylation.

Figure 2c shows the results of the immunofluorescence assay. In replicon clone 3 (Fig. 2c) and other clones (data not shown), core protein exhibited a perinuclear punctuate staining pattern, and NS3 and NS5a proteins exhibited a cytoplasmic diffuse staining pattern.

Table 2 shows the results of the immunoassay of core protein in culture medium. Figure 3a shows the results of sucrose density gradient centrifugation of the culture medium of clone 3. Core protein and HCV RNA exhibited identical peaks in a single fraction with a density of approximately 1.16 g/mL (Fig. 3a); this density is similar to that of wild-type JFH-1 virus particles.[12] This result indicates that viral particles were secreted from cells that replicated replicon RNA.

Cells inoculated with culture supernatant of full-genome replicon cell lines formed visible colonies by G418 (1 mg/mL) selection culture for 10–14 days after inoculation; these cells were fixed and stained. In the preliminary experiment, very few colonies formed (data not shown). Consequently, to increase colony formation efficiency after inoculation, the inoculated Huh7 cells were passed 1 day before seeding, culture supernatants from replicon cell lines were concentrated by ultrafiltration as described previously,[12] and inoculated cells were cultured with a lower concentration of G418 (0.3 mg/mL). These changes increased the number of colonies that formed, and colony formation by cells inoculated with supernatant of full-genome replicon cell lines occurred in a dose-dependent manner (Fig. 3b, FGR-JFH1). No colonies were formed by cells inoculated with culture supernatant of subgenomic replicon cells (Fig. 3b, SGR-JFH1).

When genomic DNA from each clone was isolated and amplified by PCR using *neo*^{r} -specific primers, we did not detect any signals (data not shown).

Long-term culture of replicon cells

Figure 4 shows the results of serial passaging of clones 3 and 5. Core protein titer of culture supernatant of clone 3 decreased rapidly at 50 days of culture. In contrast, core protein titer of culture medium of clone 5 gradually decreased throughout the observation period (Fig. 4a). HCV RNA replication levels in the cells ranged from 1.6×10^7 to 7.8×10^7 copies/μg RNA, with no significant differences between clones (Fig. 4a). Colony formation efficiency of clone 3 decreased significantly at 50 days of culture (Fig. 4b). Colony formation efficiency of clone 5 decreased gradually throughout the observation period (Fig. 4b).

Serial passages of replicon virus

The HCV RNA levels in the inoculated cells did not change significantly during the observation period

Table 1 Colony formation efficiency of JFH-1 replicon

Replicon	JFH-1 (c.f.u./μg RNA)
Subgenomic	$5.32 \times 10^4 \pm 5.02 \times 10^4$†
Full-genome	$6.59 \times 10^2 \pm 3.58 \times 10^2$

†Kato *et al.*[10] Values shown as mean ± SD.

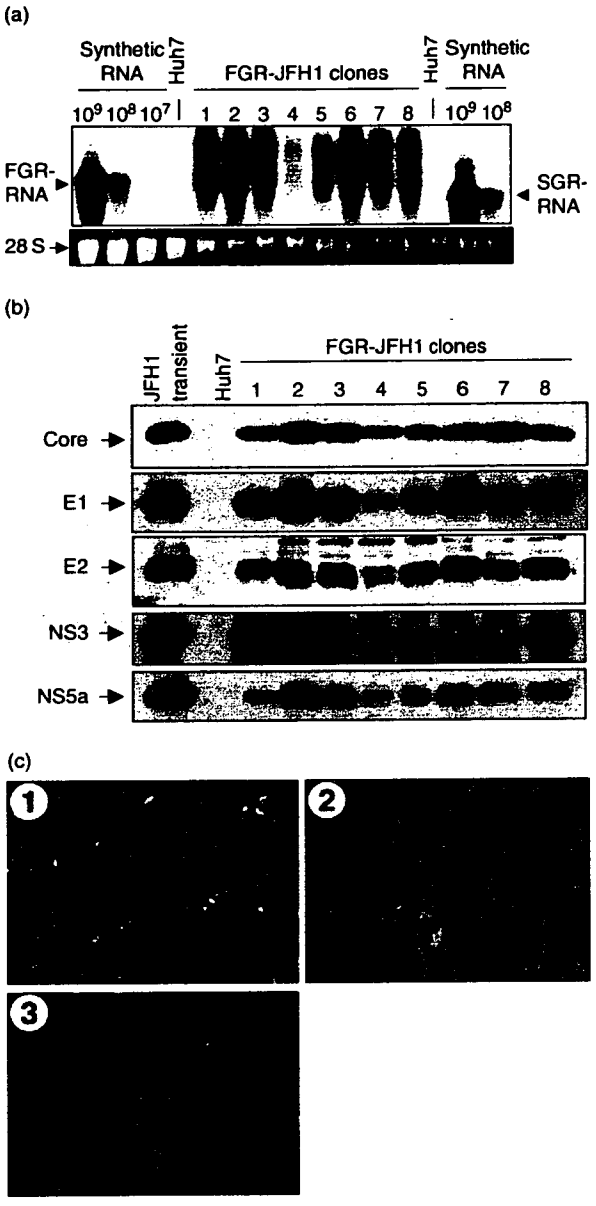

Figure 2 Analysis of isolated full-genome replicon cells. (a) Northern blot analysis of replicon RNA. Total RNA from eight isolated replicon cell clones (FGR-JFH1 clones 1–8) was analyzed by northern blotting with DNA probes of the *neo*^{r} – EMCV IRES and β-actin genes. We performed *in vitro* synthesis of 10^9, 10^8 and 10^7 copies of transcribed positive-strand full-genome replicon JFH-1 RNA (FGR-RNA) and 10^8 and 10^7 copies of positive-strand subgenomic JFH-1 replicon RNA (SGR-RNA). The synthesized RNA was loaded onto the gel as positive controls (left 3 lanes and right 2 lanes, respectively). Left and right arrowheads indicate target positions of full-genome and subgenomic replicon RNAs, respectively. Arrow indicates position of β-actin. 'Huh7' indicates cellular RNA of normal Huh7 cells, which was used as a negative control. (b) Western blot analysis. Cell lysates were prepared from clones of Huh7 cells transfected with FGR-JFH1 RNA (FGR-JFH1 clones 1–8). Huh7 cells transfected with full-length JFH-1 RNA were used as positive controls (JFH1 transient), and untransfected parental Huh7 cells (Huh7) were used as negative controls. Anti-core monoclonal antibodies and anti-E1, -E2, -NS3 and -NS5A polyclonal antibodies were used to detect HCV antigens. Target sizes of HCV proteins are indicated by arrows. (c) Subcellular localization of HCV antigens determined by immunofluorescence. Isolated FGR-JFH1 replicon cell clone 3 was cultured on cover slips. Cultured cells were fixed before being incubated with anti-Core (1, α-Core), anti-NS3 (2, α-NS3) and anti-NS5A (3, α-NS5A) antibodies. (Original magnification ×200).

(Fig. 5a). Core protein titers in culture supernatants gradually decreased in one series of the passages (Fig. 5a, Transfection 1). However, in another series (Fig. 5a, Transfection 2), core protein titer in culture supernatant increased beginning with the fourth inoculation. Colony formation of cells inoculated with culture supernatant of transfection 1 gradually decreased during the observation period. Colony formation of cells inoculated with culture supernatant of transfection 2 increased beginning with the fourth passage (Fig. 5b, P4/d118).

DISCUSSION

IN THE PRESENT study, we established a selectable, infectious full-length HCV replicon. Transcribed full-length replicon RNA was transfected into Huh7 cells. Cells transfected with the full-length replicon formed colonies at reduced efficiency, compared with cells transfected with the subgenomic replicon. However, expanded replicon cells supported efficient replicon RNA replication. Furthermore, although the replicon genome (approximately 11 kb) is longer than the wild-type genome of HCV (approximately 9.6 kb), culture supernatant from the replicon cells were infectious for naïve Huh7 cells. After long-term culture, replicon cells did not stop replicating replicon RNA, but they did stop secreting infectious viral particles. Viral adaptation might occur during repeated serial infection of the

Table 2 Mutations and titers of JFH-1 replicon

Clone	Nucleotide†	Amino acid‡	Region	Replicon RNA titer§ (copies/μg RNA)	Core protein titer¶ (fmol/L)	Colony formation efficiency†† (c.f.u./mL)
1	3893 A > C	707 Y > S	E2	2.71×10^7	64	0.3
	5610 T > A	1279 N > K	NS3			
	7236 G > A	Synonymous‡‡	NS4b			
	10161 C > A	Synonymous	NS5b			
2	None			5.19×10^7	826	63.3
3	None			4.47×10^7	3450	133.3
4	6599 A > C	1609 D > A	NS3	1.14×10^7	33	1.0
	8902 T > A	2377 S > T	NS5a			
5	9653 C > A	2627 A > E	NS5b	1.60×10^7	2904	89.3
6	None			7.09×10^7	363	15.3
7	394 C > A	Synonymous	Core§§	1.51×10^7	571	41.0
	5295 C > A	Synonymous	NS3			
	7189 T > C	1806 S > P	NS4b			
	8076 G > A	Synonymous	NS5a			
8	6483 A > G	Synonymous	NS3	1.15×10^7	387	11.3
	8972 G > A	2400 G > E	NS5a			
	9216 T > C	Synonymous	NS5b			

†Position of mutated nucleotide within replicon; ‡position of mutated amino acid within complete open reading frame of full-length JFH-1; §HCV RNA copy titer in replicon cell; ¶core protein concentration in culture supernatant of replicon cells; ††naïve Huh7 cells were inoculated with concentrated culture supernatants from replicon cells, and inoculated cells were cultured for 3 weeks in medium supplemented with G418 (0.3 mg/mL); ‡‡synonymous mutation does not change amino acid sequence; §§sequential region from 5′-untranslated region upstream of *neo*^{r} gene.

replicon virus. Importantly, selectable infection was established using HCV replicon containing full-length genotype 2a JFH-1 cDNA. This system may be useful for HCV research.

Several full-length HCV cDNAs have been cloned, and their infectivity has been confirmed *in vivo* using chimpanzee models.[15,16] However, it has been difficult to produce recombinant viral particles and test their infectivity using cell culture systems,[4,7] and this limits the ability to perform detailed analyses of the HCV life cycle and pathogenesis in cell culture. The JFH-1 strain was isolated from a patient with fulminant hepatitis, and it efficiently replicates in Huh7 cells and other hepatic and non-hepatic cell lines in subgenomic replicon form.[10,11,17] Full-length wild-type JFH-1 RNA and chimeric JFH-1 RNA can replicate in Huh7 cells and produce infectious virus.[12,18,19] Sequence analysis has revealed that the JFH-1 strain clusters with genotype 2a HCV isolates, and exhibits 89–90% homology with other genotype 2a strains at the nucleic acid level and 91–92% homology at the amino acid level.[9] The relationship between the high levels of replication and virus production of JFH-1 in cell culture is unclear. Chimeric virus, which contains structural region of J6CF strain and non-structural region from JFH-1, replicates as well as wild-type JFH-1 and produces infectious virus in cell culture.[19,20] However, wild type J6CF strain or another chimeric virus containing structural region of JFH-1 and non-structural region from J6CF did not replicate in tissue culture (unpublished data).[12] It is thus clear that non-structural proteins or genome are important for the efficient replication of JFH-1 strain.

In the present study, the full-genome JFH-1 replicon produced infectious virus particles. Full-genome replicon clones have previously been developed using genotype 1a and 1b HCV clones, but none of those replicons produced viral particles from replicon cells.[6,7,21,22] This inability to produce virus particles may be related to adaptive mutations in the replicon genome, because adaptive mutations increase replication of replicons in cultured cells. However, H77-S strain was recently reported to produce infectious virus particles into culture medium from the transfected cells, although this strain contains at least five adaptive mutations.[23] The full-length JFH-1 replicon does not require adaptive mutations to efficiently replicate in cultured cells.[10,11,17] In the present study, the full-genome replicon cells with amino acid mutations had a lower HCV RNA

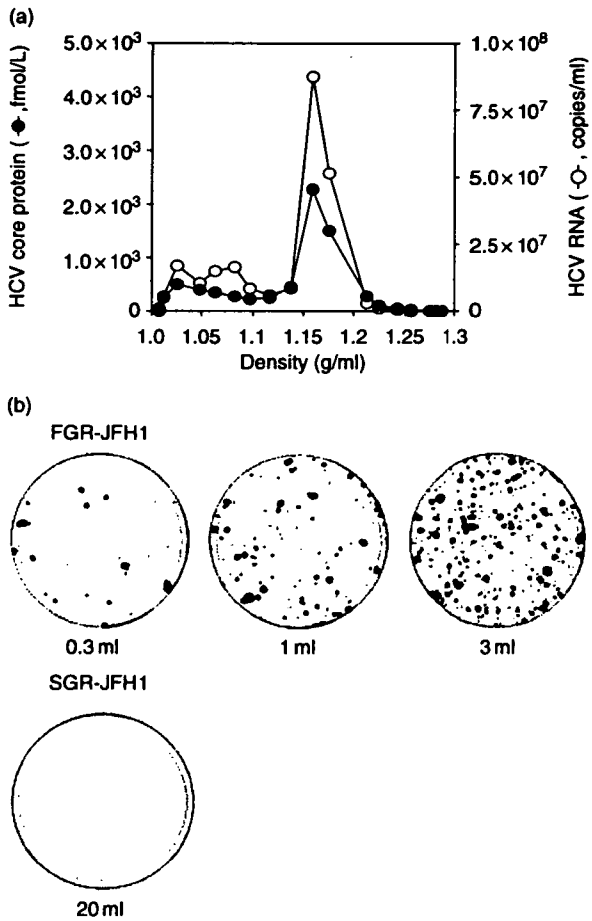

Figure 3 Analysis of culture supernatant from replicon cells. (a) Density gradient analysis. Culture supernatant from full-genome JFH-1 replicon cell clone 3 was filtered and layered on a stepwise sucrose gradient (60% to 10% wt/vol) in centrifugation tubes. After centrifugation, 22 fractions were collected from the bottom of the tubes. Core protein concentration (●) and HCV RNA titer (○) were measured in each fraction. (b) Colony formation by cells inoculated with culture supernatant from JFH-1 replicon cells. Culture supernatants from full-genome FGR-JFH1 replicon cell clone 3 and subgenomic SGR-JFH1 replicon cell clone 4-1 were cleared by centrifugation and filtration. Naïve Huh7 cells were inoculated with the cleared culture supernatant, and the inoculated cells were cultured in medium supplemented with G418 (0.3 mg/mL) for 3 weeks before staining with crystal violet. The figure shows representative staining of Huh7 cells inoculated with 0.3 mL, 1 mL and 3 mL of culture medium from FGR-JFH1 clone 3, and cells inoculated with 20 mL of medium from SGR-JFH1 clone 4-1. Before inoculation, culture media were concentrated by ultrafiltration.

titer than the full-genome replicon cells without mutations ($1.62 \times 10^7 \pm 6.43 \times 10^6$ *vs* $5.58 \times 10^7 \pm 1.35 \times 10^7$ copies/μg RNA, $P < 0.05$); however, when HCV RNA titer per cell was calculated, there was no significant difference ($5.75 \times 10^3 \pm 2.45 \times 10^3$ *vs* $8.90 \times 10^3 \pm 1.29 \times 10^3$ copies/cell, $P = 0.09$). We also determined the colony formation efficiency of replicon clones 1–8 by transfection of cellular RNA isolated from replicon cells as 1.66×10^{-6}, 1.48×10^{-6}, 3.67×10^{-7}, 8.98×10^{-7}, 5.60×10^{-7}, 1.23×10^{-6}, 1.16×10^{-6} and 7.28×10^{-7} c.f.u./RNA copy, respectively. Thus, the mutations that occurred in the full-genome of the JFH-1 replicon genome have no or slight effect of reducing RNA replication efficiency. Studies indicate that certain adaptive mutations in genotype 1 HCV replicon clones significantly increase RNA replication.[24–26] Many adaptive mutations alter the phosphorylation status of NS5A protein, and it has been reported that RNA replication efficiency is associated with NS5A phosphorylation status.[27,28] In the present study, p56 and p58 bands were observed in all the full-genome JFH-1 replicon cell clones (Fig. 2b). Thus, the high replication capacity of JFH-1 and its efficient production of infectious virus may be dependent on mechanisms other than phosphorylation of NS5A.

We previously reported incorporation of the luciferase reporter gene into a JFH-1 replicon construct and detected neutralizing antibody in chronically HCV infected patient sera.[12] In addition, Koutsoudakis *et al.* characterized the early steps of HCV infection using this luciferase reporter virus.[29] The wild-type JFH-1 genome has been shown to replicate efficiently in permissive cell lines.[18] However, an infectious, selectable full-length HCV replicon containing a neomycin-resistant gene is particularly useful for tests of the infectivity of HCV in cells with low permissiveness for HCV infection. It would be also interesting to test cell lines such as HepG2, IMY, HeLa and 293 cells, which support JFH-1 subgenomic replicon replication.[10] Recently, we also found that JFH-1 replicon can replicate in mouse cell lines.[30] These cells were not permissive for HCV infection;[12] however, they might support full-genomic replicon replication and infectious virus production. In particular, replicon cells using HeLa and 293 cells should be useful to analyze the host factors important for virus infection because these cell lines express CD81, SR-BI and LDL receptor, which are potentially important for HCV infection. In preliminary observations, full-genomic replicon could replicate in HepG2, IMY, HeLa and 293 cells, and replicon cells were established (unpublished data).

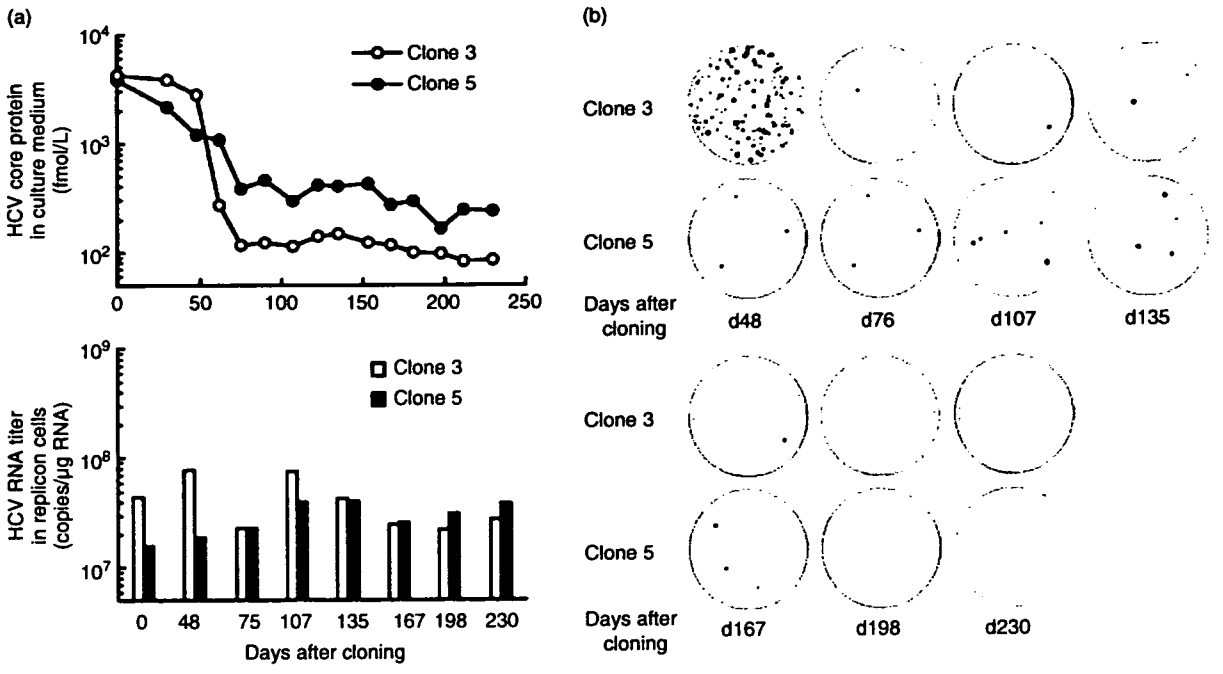

Figure 4 Long-term culture of full-genome replicon cell clones. FGR-JFH1 replicon cell clones 3 and 5 were cultured continuously for 230 days after the clones were transfected. (a) We measured the HCV core protein concentration in the culture supernatant and HCV RNA titer in replicon cells harvested at each passage. (b) We measured colony formation by naïve Huh7 cells inoculated with culture supernatant (harvested at each passage) and cultured in medium supplemented with G418 (0.3 mg/mL) for 3 weeks before staining with crystal violet.

Permissiveness for HCV infection has been shown to vary among Huh7 cell subtypes. Mutant cell lines such as Huh7.5 and Huh7.5.1 exhibit greater permissiveness than standard Huh7 cells,[18,19] whereas other Huh7 subtypes exhibit relatively low permissiveness.[12] In the present study, secretion of core protein into culture media and infectivity of culture supernatant were abolished by long-term culture of replicon cells (Fig. 4). However, long-term repeated infection of secreted replicon virus increased core protein secretion and infectivity of secreted virus, suggesting that some viruses become adapted to naïve Huh7 cells, resulting in increased secretion of infectious replicon virus (Fig. 5a, transfection 2). It is also interesting that virus replication levels were not significantly changed by repeated virus infection, which has been demonstrated to decrease the infectivity and virus secretion of some virus strains (Fig. 5a, transfection 1). Further study is needed to determine whether these differences are dependent on mutations in the virus genome or selection within infected cells. In future studies, we plan to examine mechanisms of virus adaptation to Huh7 cells and adaptive mechanisms of host cell lines.[31]

In the present study, colony formation efficiency after inoculation with culture supernatant was partly dependent on the core protein concentration of the supernatant. Colony formation efficiency for culture supernatant from clone 3 was 133.3 c.f.u./mL. The cells used in the present study were standard Huh7 cells, which are not highly permissive for HCV.[12,18] Use of cured cells such as Huh7.5 cells may increase the infection efficiency of replicon culture supernatants.[19] However, the present low infection efficiency of the replicon virus may also be due to its genomic length. The present replicon genome is about 1.5 kb longer than the wild-type HCV genome. The colony formation efficiency of the present full-genome replicon was significantly lower than that of the subgenomic replicon. The ability of viral particles to incorporate a longer genome than the wild-type genome may allow us to add other genes to the viral replicon genome, and to test expression of those genes in the infected cells.

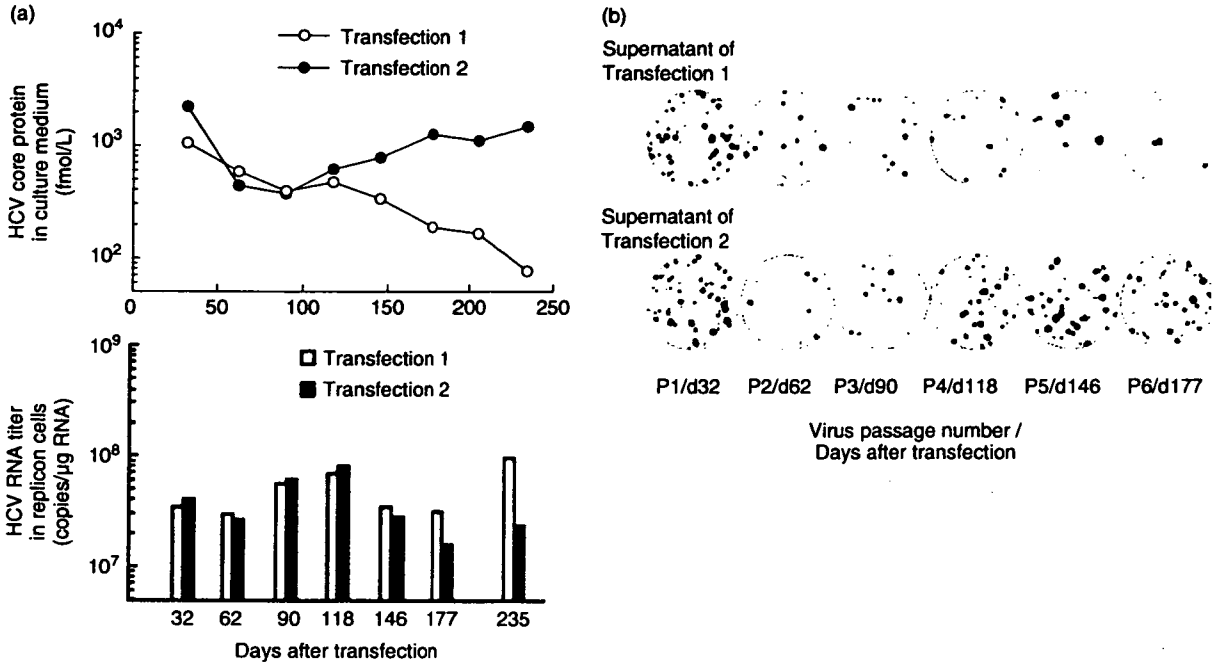

Figure 5 Repeated infection of cells with culture supernatant harvested from full-genome replicon cells. Naïve Huh7 cells were transfected with FGR-JFH1 RNA. Transfected cells were cultured for 4 weeks in medium supplemented with G418 (1 mg/mL), and culture supernatant was then harvested. New naïve Huh7 cells were inoculated with the harvested supernatant, and were then cultured in medium supplemented with G418 (0.3 mg/mL) for 4 weeks. Culture supernatant was harvested at the end of the 4 weeks, and was used to inoculate new Huh7 cells. This harvesting of supernatant, inoculation of new Huh7 cells, and incubation of the inoculated cells was repeated every 4 weeks for 235 days after transfection. Six independent experiments were performed and two representative results are shown. (a) We measured the HCV core protein concentration in culture supernatant (upper panel) and HCV RNA titer in infected cells (lower panel) harvested at each passage. (b) We measured colony formation by naïve Huh7 cells inoculated with culture supernatant (harvested at each passage) and cultured in medium supplemented with G418 (0.3 mg/mL) for 4 weeks before staining with crystal violet.

ACKNOWLEDGMENTS

THIS WORK WAS partly supported by a Grant-in-Aid for Scientific Research from the Japan Society for the Promotion of Science, grants from the Ministry of Health, Labour and Welfare of Japan, the Ministry of Education, Culture, Sports, Science and Technology of Japan, and Toray Industries Inc., and Research on Health Sciences focusing on Drug Innovation from the Japan Health Sciences Foundation.

REFERENCES

1 Choo QL, Kuo G, Weiner AJ, Overby LR, Bradley DW, Houghton M. Isolation of a cDNA clone derived from a blood-borne non-A non-B viral hepatitis genome. *Science* 1989; 244: 359–62.

2 Kuo G, Choo QL, Alter HJ *et al.* An assay for circulating antibodies to a major etiologic virus of human non-A non-B hepatitis. *Science* 1989; 244: 362–4.

3 Kiyosawa K, Sodeyama T, Tanaka E *et al.* Interrelationship of blood transfusion, non-A, non-B hepatitis and hepatocellular carcinoma: analysis by detection of antibody to hepatitis C virus. *Hepatology* 1990; 12: 671–5.

4 Bartenschlager R, Lohmann V. Replication of hepatitis C virus. *J Gen Virol* 2000; 81: 1631–48.

5 Lohmann V, Korner F, Koch J *et al.* Replication of subgenomic hepatitis C virus RNAs in a hepatoma cell line. *Science* 1999; 285: 110–13.

6 Ikeda M, Yi M, Li K, Lemon SM. Selectable subgenomic and genome-length dicistronic RNAs derived from an infectious molecular clone of the HCV-N strain of hepatitis C virus replicate efficiently in cultured Huh7 cells. *J Virol* 2002; 76: 2997–3006.

7 Pietschmann T, Lohmann V, Kaul A *et al.* Persistent and transient replication of full-length hepatitis C virus genomes in cell culture. *J Virol* 2002; 76: 4008–21.
8 Bukh J, Purcell RH, Miller RH. Sequence analysis of the core gene of 14 hepatitis C virus genotypes. *Proc Natl Acad Sci USA* 1994; 91: 8239–43.
9 Kato T, Furusaka A, Miyamoto M *et al.* Sequence analysis of hepatitis C virus isolated from a fulminant hepatitis patient. *J Med Virol* 2001; 64: 334–9.
10 Kato T, Date T, Miyamoto M *et al.* Efficient replication of the genotype 2a hepatitis C virus subgenomic replicon. *Gastroenterology* 2003; 125: 1808–17.
11 Date T, Kato T, Miyamoto M *et al.* Genotype 2a hepatitis C virus subgenomic replicon can replicate in HepG2 and IMY-N9 cells. *J Biol Chem* 2004; 279: 22371–6.
12 Wakita T, Pietschmann T, Kato T *et al.* Production of infectious hepatitis C virus in tissue culture from a cloned viral genome. *Nat Med* 2005; 11: 791–6.
13 Aoyagi K, Ohue C, Iida K *et al.* Development of a simple and highly sensitive enzyme immunoassay for hepatitis C virus core antigen. *J Clin Microbiol* 1999; 37: 1802–8.
14 Takeuchi T, Katsume A, Tanaka T *et al.* Real-time detection system for quantification of hepatitis C virus genome. *Gastroenterology* 1999; 116: 636–42.
15 Kolykhalov AA, Agapov EV, Blight KJ, Mihalik K, Feinstone SM, Rice CM. Transmission of hepatitis C by intrahepatic inoculation with transcribed RNA. *Science* 1997; 277: 570–4.
16 Yanagi M, Purcell RH, Emerson SU, Bukh J. Transcripts from a single full-length cDNA clone of hepatitis C virus are infectious when directly transfected into the liver of a chimpanzee. *Proc Natl Acad Sci USA* 1997; 94: 8738–43.
17 Kato T, Date T, Miyamoto M, Zhao Z, Mizokami M, Wakita T. Nonhepatic cell lines HeLa and 293 support efficient replication of the hepatitis C virus genotype 2a subgenomic replicon. *J Virol* 2005; 79: 592–6.
18 Zhong J, Gastaminza P, Cheng G *et al.* Robust hepatitis C virus infection in vitro. *Proc Natl Acad Sci USA* 2005; 102: 9294–9.
19 Lindenbach BD, Evans MJ, Syder AJ *et al.* Complete replication of hepatitis C virus in cell culture. *Science* 2005; 309: 623–6.
20 Pietschmann T, Kaul A, Koutsoudakis G *et al.* Construction and characterization of infectious intragenotypic and intergenotypic hepatitis C virus chimeras. *Proc Natl Acad Sci USA* 2006; 103: 7408–13.
21 Blight KJ, McKeating JA, Rice CM. Highly permissive cell lines for subgenomic and genomic hepatitis C virus RNA replication. *J Virol* 2002; 76: 13001–14.
22 Blight KJ, McKeating JA, Marcotrigiano J, Rice CM. Efficient replication of hepatitis C virus genotype 1a RNAs in cell culture. *J Virol* 2003; 77: 3181–90.
23 Yi M, Villanueva RA, Thomas DL, Wakita T, Lemon SM. Production of infectious genotype 1a hepatitis C virus (Hutchinson strain) in cultured human hepatoma cells. *Proc Natl Acad Sci USA* 2006; 103: 2310–15.
24 Blight KJ, Kolykhalov AA, Rice CM. Efficient initiation of HCV RNA replication in cell culture. *Science* 2000; 290: 1972–4.
25 Lohmann V, Korner F, Dobierzewska A, Bartenschlager R. Mutations in hepatitis C virus RNAs conferring cell culture adaptation. *J Virol* 2001; 75: 1437–49.
26 Krieger N, Lohmann V, Bartenschlager R. Enhancement of hepatitis C virus RNA replication by cell culture-adaptive mutations. *J Virol* 2001; 75: 4614–24.
27 Evans MJ, Rice CM, Goff SP. Phosphorylation of hepatitis C virus nonstructural protein 5A modulates its protein interactions and viral RNA replication. *Proc Natl Acad Sci USA* 2004; 101: 13038–43.
28 Appel N, Pietschmann T, Bartenschlager R. Mutational analysis of hepatitis C virus nonstructural protein 5A: potential role of differential phosphorylation in RNA replication and identification of a genetically flexible domain. *J Virol* 2005; 79: 3187–94.
29 Koutsoudakis G, Kaul A, Steinmann E *et al.* Characterization of the early steps of hepatitis C virus infection by using luciferase reporter viruses. *J Virol* 2006; 80: 5308–20.
30 Uprichard SL, Chung J, Chisari FV, Wakita T. Replication of a hepatitis C virus replicon clone in mouse cells. *Virol J* 2006; 3: 89.
31 Bartenschlager R, Pietschmann T. Efficient hepatitis C virus cell culture system: what a difference the host cell makes. *Proc Natl Acad Sci USA* 2005; 102: 9739–40.

JOURNAL OF VIROLOGY, Feb. 2007, p. 1174–1185 Vol. 81, No. 3
0022-538X/07/$08.00+0 doi:10.1128/JVI.01684-06

E6AP Ubiquitin Ligase Mediates Ubiquitylation and Degradation of Hepatitis C Virus Core Protein▽

Masayuki Shirakura,[1] Kyoko Murakami,[1] Tohru Ichimura,[2] Ryosuke Suzuki,[1] Tetsu Shimoji,[1] Kouichirou Fukuda,[1] Katsutoshi Abe,[1] Shigeko Sato,[3] Masayoshi Fukasawa,[3] Yoshio Yamakawa,[3] Masahiro Nishijima,[3] Kohji Moriishi,[4] Yoshiharu Matsuura,[4] Takaji Wakita,[1] Tetsuro Suzuki,[1] Peter M. Howley,[5] Tatsuo Miyamura,[1] and Ikuo Shoji[1]*

Department of Virology II[1] and Department of Biochemistry and Cell Biology,[3] National Institute of Infectious Diseases, Shinjuku-ku, Tokyo 162-8640, Japan; Department of Chemistry, Graduate School of Science, Tokyo Metropolitan University, Hachioji-shi, Tokyo 192-0397, Japan[2]; Department of Molecular Virology, Research Institute for Microbial Diseases, Osaka University, Osaka 565-0871, Japan[4]; and Department of Pathology, Harvard Medical School, 77 Avenue Louis Pasteur, Boston, Massachusetts 02115[5]

Received 4 August 2006/Accepted 8 November 2006

Hepatitis C virus (HCV) core protein is a major component of viral nucleocapsid and a multifunctional protein involved in viral pathogenesis and hepatocarcinogenesis. We previously showed that the HCV core protein is degraded through the ubiquitin-proteasome pathway. However, the molecular machinery for core ubiquitylation is unknown. Using tandem affinity purification, we identified the ubiquitin ligase E6AP as an HCV core-binding protein. E6AP was found to bind to the core protein in vitro and in vivo and promote its degradation in hepatic and nonhepatic cells. Knockdown of endogenous E6AP by RNA interference increased the HCV core protein level. In vitro and in vivo ubiquitylation assays showed that E6AP promotes ubiquitylation of the core protein. Exogenous expression of E6AP decreased intracellular core protein levels and supernatant HCV infectivity titers in the HCV JFH1-infected Huh-7 cells. Furthermore, knockdown of endogenous E6AP by RNA interference increased intracellular core protein levels and supernatant HCV infectivity titers in the HCV JFH1-infected cells. Taken together, our results provide evidence that E6AP mediates ubiquitylation and degradation of HCV core protein. We propose that the E6AP-mediated ubiquitin-proteasome pathway may affect the production of HCV particles through controlling the amounts of viral nucleocapsid protein.

Hepatitis C virus (HCV; a single-stranded, positive-sense RNA virus that is classified in the family *Flaviviridae*) is the main cause of chronic hepatitis, liver cirrhosis, and hepatocellular carcinoma (5, 26, 45). More than 170 million people worldwide are chronically infected with HCV (41). The approximately 9.6-kb HCV genome encodes a unique open reading frame that is translated into a polyprotein (5, 54). The polyprotein is cleaved cotranslationally into at least 10 proteins by viral proteases and cellular signalases (6, 10).

The HCV core protein represents the first 1 to 191 amino acids (aa) of the polyprotein and is followed by two glycoproteins, E1 and E2 (6). The core protein plays a central role in the packaging of viral RNA (25, 40); modulates various cellular processes, including signal transduction pathways, transcriptional control, cell cycle progression, apoptosis, lipid metabolism, and the immune response (9, 40); and has transforming potential in certain cells (43). Mice transgenic for the HCV core gene develop steatosis (32) and later hepatocellular carcinoma (31). These findings suggest that HCV core protein plays a crucial role in hepatocarcinogenesis.

Two major forms of the HCV core protein, p21 (mature form) and p23 (immature form), can be generated in cultured cells (60). Cellular signal peptidase cleaves at the junction of the core/E1, releasing the immature form of the core protein from the polypeptide (12, 46). Signal peptide peptidase cleaves just before the signal sequence, liberating the mature form of the HCV core protein at the cytoplasmic face of the endoplasmic reticulum (29). Several different sites have been proposed as potential cleavage sites of signal peptide peptidase, such as Leu-179 (15, 29), Phe-177 (36, 37), Leu-182 (15), and Ser-173 (46). Further processing of the HCV core protein yields a 17-kDa product with a C terminus at around amino acid 152. A truncated form of the core protein, p17, was found in transfected cells (42, 52) and liver tissues from humans with hepatocellular carcinoma (59). The majority of this protein translocates to the nucleus. The C terminus of the core protein is important for regulating the stability of the protein (20, 52).

We previously showed that the C-terminally truncated forms of the core protein are degraded through the ubiquitin-proteasome pathway (52). We found that the mature form of the core protein, p21, also links to a few ubiquitin moieties, suggesting that the ubiquitin-proteasome pathway involves proteolysis of heterologous species of the core protein (52). Overexpression of PA28γ (a REG family proteasome activator also known as REGγ or Ki antigen) enhances the proteasomal degradation of the HCV core protein (30). A recent study has shown that

* Corresponding author. Mailing address: Department of Virology II, National Institute of Infectious Diseases, 1-23-1 Toyama, Shinjuku-ku, Tokyo 162-8640, Japan. Phone: 81 3-5285-1111. Fax: 81 3-5285-1161. E-mail: ishoji@nih.go.jp.
▽ Published ahead of print on 15 November 2006.

PA28γ is involved in the degradation of the steroid receptor coactivator 3 (SRC-3) in an ATP- and ubiquitin-independent manner (27). It is still unclear what E3 ubiquitin ligase is responsible for ubiquitylation of the HCV core protein.

E6AP was initially identified as the cellular factor that stimulates ubiquitin-mediated degradation of the tumor suppressor p53 in conjunction with the E6 protein of cancer-associated human papillomavirus types 16 and 18 (14, 48). The E6-E6AP complex functions as a E3 ubiquitin ligase in the ubiquitylation of p53 (49). E6AP is the prototype of a family of ubiquitin ligases called HECT domain ubiquitin ligases, all of which contain a domain *h*omologous to the *E6AP c*arboxyl *t*erminus (13). Interestingly, E6AP is not involved in the regulation of p53 ubiquitylation in the absence of E6 (55). Several potential E6-independent substrates for E6AP have been identified, such as hHR23A, Blk, and Mcm7 (23, 24, 35). E6AP is also a candidate gene for Angelman syndrome, which is a severe neurological disorder characterized by mental retardation (21).

This study aimed to identify endogenous ubiquitin-proteasome pathway proteins that are associated with HCV core protein. Tandem affinity purification and mass spectrometry analysis identified E6AP as an HCV core-binding protein. Here we present evidence that E6AP associates with HCV core protein in vitro and in vivo and is involved in ubiquitylation and degradation of HCV core protein. We propose that an E6AP-mediated ubiquitin-proteasome pathway may affect the production of HCV particles through controlling the amounts of HCV core protein.

MATERIALS AND METHODS

Cell culture and transfection. Human embryonic kidney 293T cells, human hepatoblastoma HepG2 cells, and human hepatoma Huh-7 cells were cultured in Dulbecco's modified Eagle's medium (Sigma) supplemented with 50 IU/ml penicillin, 50 μg/ml streptomycin (Invitrogen), and 10% (vol/vol) fetal bovine serum (JRH Biosciences) at 37°C in a 5% CO_2 incubator. 293T cells and HepG2 cells were transfected with plasmid DNA using FuGene 6 transfection reagents (Roche). Huh-7 cells were transfected with plasmid DNA using *Trans*IT LT1 transfection reagents (Mirus).

Plasmids and recombinant baculoviruses. MEF tag cassette (containing *myc* tag, the tobacco *e*tch virus protease cleavage site, and *FLAG* tag) (16) was fused to the N terminus of the cDNA encoding core protein of HCV NIHJ1 (genotype 1b) (1). To express MEF-tagged core protein in mammalian cells, the genome coding for HCV core protein (amino acids 1 to 191) was amplified by PCR using pBR HCV NIHJ1 as a template. Sense oligonucleotide containing a Kozak consensus translation initiation codon and antisense oligonucleotide containing an in-frame translation stop codon were synthesized by PCR. The amplified PCR product was purified, digested with EcoRI and EcoRV, and then inserted into the EcoRI-EcoRV site of pcDNA3-MEF. FLAG-tagged HCV core expression plasmids based upon pCAGGS (34) were described previously (30). To express E6AP and the active-site cysteine-to-alanine mutant of E6AP in mammalian cells, pCMV4-HA-E6AP isoform II and pCMV4-HA-E6AP C-A were utilized (19). The C-A mutation was introduced at the site of E6AP C843. To express E6AP and E6AP C-A under the CAG promoter, the E6AP fragment and the E6AP C-A fragment were amplified by PCR, purified, digested with SmaI and NotI, and blunt ended using a DNA blunting kit (Takara). These PCR fragments were subcloned into pCAGGS.

To make a fusion protein consisting of glutathione *S*-transferase (GST) fused to the N terminus of E6AP in *Escherichia coli*, the E6AP fragment was amplified by PCR and the resultant product was cloned into the SmaI-NotI site of pGEX4T-1 vector (Amersham Biosciences). To express a series of E6AP truncation mutants as GST fusion proteins, each fragment was amplified by PCR and cloned into the SmaI-NotI site of pGEX4T-1. To purify GST core protein efficiently by two-step affinity purification, we fused hexahistidine (His) tag to the C terminus of GST fusion proteins. To bacterially express HCV core (aa 1 to 173) protein as a fusion protein containing N-terminal GST tag and C-terminal His tag, core fragment was amplified by PCR and the resultant product was cloned into the EcoRI-NotI site of pGEX4T-1 vector. The resultant plasmid was designated pGEX GST-C173HT. To express GST core (1–152)-His and GST-His in *E. coli*, pGEX core (1–152)-His and pGEX-His were constructed similarly. The resultant plasmids were designated pGEX GST-C152HT and pGEX GST-HT, respectively.

To generate recombinant baculoviruses expressing GST-E6AP, GST-E6AP fragment was excised from pGEX E6AP by digestion with SmaI and Tth111I and ligated into the SmaI-Tth111I site of pVL1392 (Invitrogen). To express GST-E6AP C-A, pVLGST-E6AP C-A was constructed similarly. To generate recombinant baculovirus expressing HCV core (aa 1 to 173) protein as a fusion protein containing N-terminal GST tag and C-terminal His tag, GST-C173HT fragment was amplified by PCR using pGEX GST-C173HT as a template, digested with BglII-XbaI, and subcloned into the BglII-XbaI site of pVL1392. To generate recombinant baculoviruses expressing GST-C152HT and GST-HT, cDNA fragments corresponding to GST-C152HT and GST-HT were amplified by PCR and subcloned into pVL1392, respectively. The resultant plasmids were designated pVLGST-C173HT, pVLGST-C152HT, and pVLGST-HT. To generate recombinant baculovirus expressing MEF-tagged E6AP, cDNA fragment encoding MEF-E6AP was subcloned into pVL1392. To express HCV core protein in the TNT-coupled wheat germ lysate system (Promega), HCV core cDNA was inserted in the EcoRI site of pCMVTNT (Promega). The primer sequences used in this study are available from the authors upon request. The sequences of the inserts were extensively verified using an ABI PRISM 3100-Avant Genetic Analyzer (Applied Biosystems). Recombinant baculoviruses were recovered using a BaculoGold transfection kit (Pharmingen) according to the manufacturer's instructions.

Antibodies. The mouse monoclonal antibodies (MAbs) used in this study were anti-hemagglutinin (anti-HA) MAb (12CA5; Roche), anti-FLAG (M2) MAb (Sigma), anti-c-*myc* MAb (9E10; Santa Cruz), anti-glyceraldehyde-3-phosphate dehydrogenase (anti-GAPDH) MAb (Chemicon), anti-GST MAb (Santa Cruz), anti-ubiquitin MAb (Chemicon), anti-E6AP MAb (E6AP-330) (Sigma), anticore MAb (B2; Anogen), and another anti-core MAb (2H9) (56). Polyclonal antibodies (PAbs) used in this study were anti-HA rabbit PAb (Y-11; Santa Cruz), anti-FLAG rabbit PAb (F7425; Sigma), anti-E6AP rabbit PAb (H-182; Santa Cruz), anti-DDX3 rabbit PAb (47), anti-PA28γ rabbit PAb (Affiniti), and anti-GST goat PAb (Amersham). Anticore rabbit PAb (TS1) was raised against the recombinant GST core protein.

MEF purification procedure. 293T cells were transfected with the plasmid expressing MEF core by the calcium phosphate precipitation method (4). After the cells were lysed, the expressed MEF core and its binding proteins were recovered following the procedure described previously (16). 293T cells transfected with pcDNA3-MEF core in four 10-cm dishes were lysed in 2 ml of lysis buffer: 50 mM Tris-HCl (pH 7.5), 150 mM NaCl, 10% (wt/vol) glycerol, 100 mM NaF, 1 mM Na_3VO_4, 1% (wt/vol) Triton X-100, 5 μM $ZnCl_2$, 2 mM phenylmethylsulfonyl fluoride, 10 μg/ml aprotinin, and 1 μg/ml leupeptin. The lysate was centrifuged at 100,000 × *g* for 20 min at 4°C. The supernatant was passed through a 5-μm filter, incubated with 100 μl of Sepharose beads for 60 min at 4°C, and then passed through a 0.65-μm filter. The filtered supernatant was mixed with 100 μl of anti-myc-conjugated Sepharose beads for the first immunoprecipitation. After incubation for 90 min at 4°C, the beads were washed five times with 1 ml of TNTG buffer (20 mM Tris-HCl, pH 7.5, 150 mM NaCl, 10% [wt/vol] glycerol, and 1% [wt/vol] Triton X-100), twice with 1 ml of buffer A (20 mM Tris-HCl, pH 7.5, 150 mM NaCl, and 1% [wt/vol] Triton X-100), and finally once with 1 ml of TNT buffer (50 mM Tris-HCl, pH 8.0, 150 mM NaCl, 1% [wt/vol] Triton X-100). The washed beads were incubated with 10 U of tobacco etch virus protease (Invitrogen) in TNT buffer (100 μl) to release bound protein complexes from the beads. After incubation for 60 min at room temperature, the supernatant was pooled and the beads were washed twice with 70 μl of buffer A. The resulting supernatants were combined and incubated with 12 μl of FLAG-Sepharose beads for the second immunoprecipitation. After incubation for 60 min at room temperature, the beads were washed three times with 240 μl of buffer A, and proteins bound to the immobilized HCV core protein on the FLAG beads were dissociated by incubation with 80 μg/ml FLAG peptide (NH_2-Asp-Tyr-Lys-Asp-Asp-Asp-Asp-Lys-COOH) (Sigma).

MS/MS. Proteins were separated by 9% sodium dodecyl sulfate-polyacrylamide gel electrophoresis (SDS-PAGE) and visualized by silver staining. The stained bands were excised and digested in the gel with lysylendoprotease-C (Lys-C), and the resulting peptide mixtures were analyzed using a direct nanoflow liquid chromatography-tandem mass spectrometry (MS/MS) system (33), equipped with an electrospray interface reversed-phase column, a nanoflow gradient device, a high-resolution Q-time of flight hybrid mass spectrometer (Q-TOF2; Micromass), and an automated data analysis system. All the MS/MS

spectra were searched against the nonredundant protein sequence database maintained at the National Center for Biotechnology Information using the Mascot program (Matrixscience) to identify proteins. The MS/MS signal assignments were also confirmed manually.

Expression and purification of recombinant proteins. *E. coli* BL21(DE3) cells were transformed with plasmids expressing GST fusion protein or His-tagged protein and grown at 37°C. Expression of the fusion protein was induced by 1 mM isopropyl-β-D-thiogalactopyranoside at 37°C for 4 h. Bacteria were harvested, suspended in lysis buffer (phosphate-buffered saline [PBS] containing 1% Triton X-100), and sonicated on ice.

Hi5 cells were infected with recombinant baculoviruses to produce GST-C173HT, GST-C152HT, GST-HT, MEF-E6AP, and His-tagged mouse E1 (17). GST and GST fusion proteins were purified on glutathione-Sepharose beads (Amersham Bioscience) according to the manufacturer's protocols. His-tagged proteins were purified on nickel-nitrilotriacetic acid beads (QIAGEN) according to the manufacturer's protocols. MEF-E6AP and MEF-E6AP C-A were purified on anti-FLAG M2 agarose beads (Sigma) according to the manufacturer's protocols.

Immunoblot analysis. Immunoblot analysis was performed essentially as described previously (11). The membrane was visualized with SuperSignal West Pico chemiluminescent substrate (Pierce).

HCV core protein and E6AP binding assays. To map the E6AP binding site on HCV core protein, 2.5 μg of purified recombinant GST-E6AP expressed in Hi5 cells was mixed with 1,000 μg of 293T cell lysates transfected with a series of FLAG-tagged HCV core deletion mutants as indicated. The protein concentration of the cells was determined using the bicinchoninic acid protein assay kit (Pierce). The mixtures were immunoprecipitated with anti-FLAG M2 agarose beads (Sigma), and proteins bound to the immobilized HCV core protein on anti-FLAG beads were dissociated with FLAG peptide (Sigma). The eluates were analyzed by immunoblotting with anti-GST PAb. To map the HCV core-binding site on E6AP, GST pull-down assays were performed as described previously (51).

In vivo ubiquitylation assay. In vivo ubiquitylation assays were performed essentially as described previously (57). FLAG-core was immunoprecipitated with anti-FLAG beads. Immunoprecipitates were analyzed by immunoblotting, using either anti-HA PAb or anticore PAb (TS1) to detect ubiquitylated core proteins.

In vitro ubiquitylation assay. For in vitro ubiquitylation of HCV core protein, purified GST-C173HT and GST-C152HT were used as substrates. Purified GST-HT was used as a negative control. Assays were done in 40-μl volumes containing 20 mM Tris-HCl, pH 7.6, 50 mM NaCl, 5 mM ATP, 10 mM $MgCl_2$, 8 μg of bovine ubiquitin (Sigma), 0.1 mM dithiothreitol, 200 ng mouse E1, 200 ng E2 (UbcH7), and 0.5 μg each of MEF-E6AP or MEF-E6AP C-A. The reaction mixtures were incubated at 37°C for 120 min followed by purification with glutathione-Sepharose beads and immunoblotting with the indicated antibodies.

siRNA transfection. 293T cells or Huh-7 cells at 3×10^5 cells in a six-well plate were transfected with 40 pmol of either E6AP-specific short interfering RNA (siRNA; Sigma) or scramble negative-control siRNA duplexes (Sigma) using HiPerFect transfection reagent (QIAGEN) following the manufacturer's instructions. The siRNA target sequences were as follows: E6AP (sense), 5′-GGGUC UACACCAGAUUGCUTT-3′; scramble negative control (sense), 5′-UUGCG GGUCUAAUCACCGATT-3′.

CHX half-life experiments. To examine the half-life of HCV core protein, transfected 293T cells were treated with 50 μg/ml cycloheximide (CHX) at 44 h posttransfection. The cells at zero time points were harvested immediately after treatment with CHX. Cells from subsequent time points were incubated in medium containing CHX at 37°C for 3, 6, and 9 h as indicated.

Infection of Huh-7 cells with secreted HCV. Infectious HCV JFH1 was produced in Huh-7.5.1 cells (61) as described previously (56). Culture supernatant containing infectious HCV JFH1 was collected and passed through a 0.22-μm filter. Naïve Huh-7 cells were seeded 24 h before infection at a density of 1×10^6 in a 10-cm dish. The cells were incubated with 2.5 ml of the inoculum (6.5×10^3 50% tissue culture infectious dose [$TCID_{50}$]/ml) for 3 h, washed three times with PBS, and supplemented with fresh complete Dulbecco's modified Eagle's medium. Then the cells were transfected with 6 μg each of pCAGGS, pCAG-HA-E6AP, or pCAG-HA-E6AP C-A by using TransIT LT1 (Mirus). The cells were trypsinized and replated in six-well plates at 1 day postinfection. The culture medium was changed every 2 days. The culture supernatants and the cells were collected at days 3 and 7 postinfection.

Quantitation of HCV RNA and core protein. We quantitated HCV core protein in cell lysate using the HCV core antigen enzyme-linked immunosorbent assay (ELISA) (Ortho-Clinical Diagnostics). Total RNA was extracted from cells using TRIzol reagent (Invitrogen). To quantitate HCV RNAs, real-time reverse transcription-PCR was performed as described previously (53).

Infectivity assay. The $TCID_{50}$ was calculated essentially based on the method described previously (28). Virus titration was performed by seeding Huh-7 cells in 96-well plates at 1×10^4 cells/well. Samples were serially diluted fivefold in complete growth medium and used to infect the seeded cells (six wells per dilution). Following 3 days of incubation, the cells were immunostained for core with anticore MAb (2H9). Wells that expressed at least one core-expressing cell were counted as positive, and the $TCID_{50}$ was calculated.

Immunocytochemistry and fluorescence microscopy. Cells on collagen-coated coverslips were washed with PBS, fixed with 4% paraformaldehyde for 30 min at 4°C, and permeabilized with PBS containing 0.2% Triton X-100. Cells were preincubated with BlockAce (Dainippon Pharmaceuticals), incubated with specific antibodies as primary antibodies, washed, and incubated with rhodamine-conjugated goat anti-rabbit immunoglobulin G (ICN Pharmaceuticals, Inc.) and Qdot 565-conjugated goat anti-mouse immunoglobulin G (Quantumdot) as secondary antibody. Then the cells were washed with PBS, counterstained with DAPI (4′,6′-diamidino-2-phenylindole) solution (Sigma) for 3 min, mounted on glass slides, and examined with a BZ-8000 microscope (Keyence).

Knockdown of endogenous E6AP in HCV JFH1-infected Huh-7 cells. Naïve Huh-7 cells at 10^6 cells/10-cm dish were inoculated with 2.5 ml of the inoculum including infectious HCV JFH1 (6.5×10^3 $TCID_{50}$/ml) and cultured. The cells were replated in a six-well plate at 3×10^5 cells/well at day 11 postinfection and transfected with 40 pmol of E6AP siRNA or control siRNA. The culture medium was changed at 24 h after transfection. The cells were harvested at day 2 after transfection, and the intracellular core protein levels were quantitated using the HCV core antigen ELISA. The culture supernatants were collected at day 2 after transfection and assayed for $TCID_{50}$ determinations.

RESULTS

Identification of E6AP as an HCV core-binding protein. To identify the molecular machinery for HCV core ubiquitylation, we searched for endogenous ubiquitin-proteasome pathway proteins that associated with HCV core protein. HCV core-binding proteins (i.e., MEF core and its binding proteins, recovered from lysed cells) were purified by a tandem affinity purification procedure using a tandem tag (known as MEF tag) (16). Ten proteins were reproducibly detected (Fig. 1A, lane 2), but none were recovered from lysed control cells transfected with empty vector alone (Fig. 1A, lane 1).

To identify the proteins, silver-stained bands were excised from the gel, digested by Lys-C, and analyzed using a direct nanoflow liquid chromatography-MS/MS system. Nine proteins were identified: two known HCV core-binding proteins, human DEAD box protein DDX3 (38) and proteasome activator PA28γ (30), and seven potential HCV core-binding proteins. E6AP was identified (Fig. 1A, lane 2) on the basis of five independent MS/MS spectra (Table 1). Immunoblot analyses confirmed the proteomic identification of E6AP, DDX3, PA28γ, and MEF-core (Fig. 1B to E).

E6AP binding domain for HCV core protein. The E6AP binding domain for HCV core protein was investigated. Figure 2A is a schematic representation of E6AP and known motifs in E6AP. A series of deletion mutants of E6AP as GST fusion proteins were expressed in *E. coli*. GST pull-down assays found that the carboxyl-terminal deletion mutant E6AP (1–517), but not E6AP (1–418) (Fig. 2C, lanes C and D), and the amino-terminal deletion mutant E6AP (418–875), but not E6AP (517–875) (Fig. 2C, lanes J and K), were able to bind to the core protein. The signal was absent when unprogrammed wheat germ extracts (the negative control) were used as a source of proteins (data not shown). GST pull-down assays (Fig. 2B) found that the region from aa 418 to aa 517 is important for binding to the HCV core protein. An assay of the

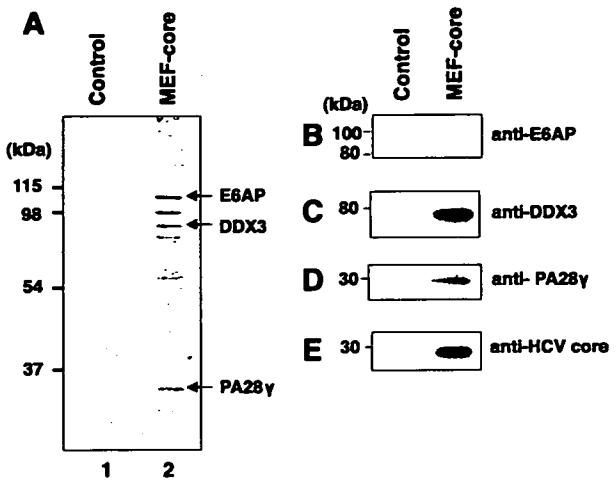

FIG. 1. HCV core protein associates with E6AP in vivo. (A) 293T cells were transfected with pcDNA3-MEF-core or empty plasmid, incubated for 48 h, and then harvested. The expressed MEF-core and binding proteins were recovered using the MEF purification procedure. Proteins bound to the MEF-core immobilized on anti-FLAG beads were dissociated with FLAG peptides, resolved by 9% SDS-PAGE, and visualized by silver staining. Control experiments were performed using 293T cells transfected with vector alone. The positions of E6AP, DDX3, and PA28γ are indicated by arrows. (B to E) The proteins detected in panel A were confirmed by immunoblotting with appropriate antibodies: E6AP (B), DDX3 (C), PA28γ (D), and MEF-core (E).

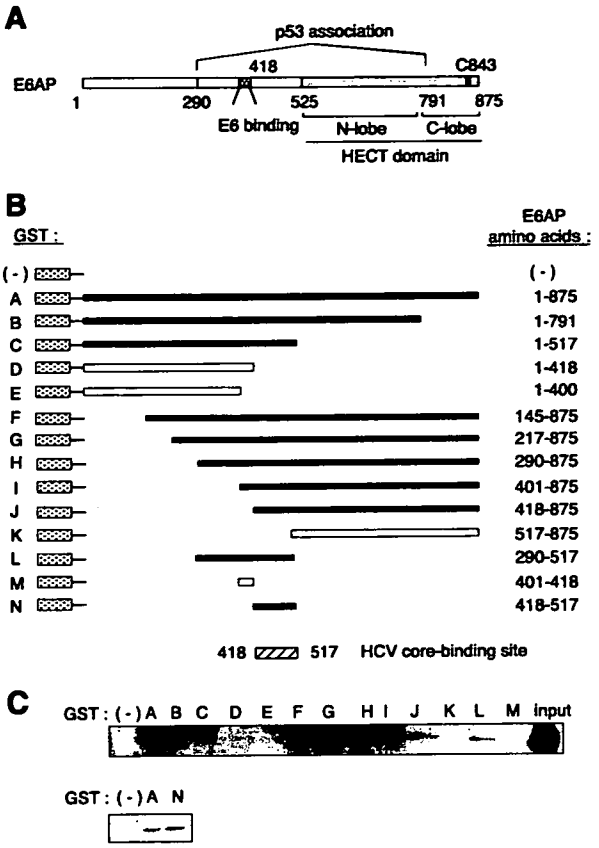

FIG. 2. Mapping of the HCV core-binding domain for E6AP. (A) Structure of E6AP. Shown is a schematic representation of the regions of E6AP isoform II that mediate E6 binding (aa 401 to 418), E6-dependent association with p53 (aa 290 to 791), and the HECT catalytic domain (aa 525 to 875). The catalytic cysteine residue is located at aa 843. (B) Schematic representation of GST-E6AP proteins. GST proteins A through N contain the E6AP amino acids indicated to the right. The shaded region of each represents the GST sequence. Closed boxes represent proteins that are bound specifically to HCV core protein, and open boxes represent those that are not bound. (C) Binding of HCV core protein to GST-E6AP proteins A through N. In vitro-translated core protein (aa 1 to 173) was assayed for association with GST (-) or the GST-E6AP fusion proteins A through N. Association of core protein was detected by immunoblotting with anti-core MAb.

ability of GST-E6AP (418–517) to bind to the HCV core protein was confirmatory (Fig. 2C, lane N) and led to the conclusion that the HCV core-binding domain of E6AP was aa 418 to aa 517.

The HCV core-binding domain for E6AP. By use of a panel of HCV core deletion mutants (Fig. 3A), GST-E6AP was found to coimmunoprecipitate with all of the FLAG-core proteins (Fig. 3A, lanes A to H) except FLAG-core (72–191) or FLAG-core (92–191) (Fig. 3A, lanes I and J). No association of control GST protein with any FLAG-core proteins was observed (data not shown). These data suggest that the aa-58-to-aa-71 segment of the HCV core binds to E6AP. The ability of GST-core (58–71) to associate with purified MEF-E6AP confirmed that the core (aa 58–71) was the site for E6AP binding on the HCV core protein (Fig. 3B).

E6AP decreases steady-state levels of HCV core protein in 293T cells and HepG2 cells. One of the features of HECT domain ubiquitin ligases is direct association with their substrates (50). Thus, we hypothesized that E6AP would function as an E3 ubiquitin ligase for the HCV core protein. We assessed the effects of E6AP on the HCV core protein in 293T cells. FLAG-core (1–191) together with HA-tagged wild-type E6AP, catalytically inactive mutant E6AP, E6AP C-A (19), or WWP1 (another HECT domain ubiquitin ligase) (22) was introduced into 293T cells, and the levels of the core protein were examined by immunoblotting. The steady-state levels of the core protein decreased with an increase in the amount of E6AP plasmids (Fig. 4A and B). However, neither E6AP C-A mutant nor WWP1 decreased the steady-state levels of the core protein, suggesting that E6AP enhances degradation of the core protein.

To verify the critical need for endogenous E6AP in the core degradation, expression of E6AP was knocked down by siRNA and the expression of the core protein and E6AP was assayed by immunoblotting. Transfection of the E6AP-specific siRNA

TABLE 1. Identification of E6AP by tandem mass spectrometry[a]

Peptide *m/z*	Sequence determined	Residues
720.9	VFSSAEALVQSFR	156–168
922.4	AACSAAAMEEDSEASSSR	196–213
774.9	MMETFQQLITYK	339–350
1,053.1	ITVLYSLVQGQQLNPYLR	507–524
809.4	EFVISYSDYILNK	712–724

[a] The protein was ubiquitin protein ligase E3A (E6AP) isoform 2 (GenBank accession no. NP_000453).

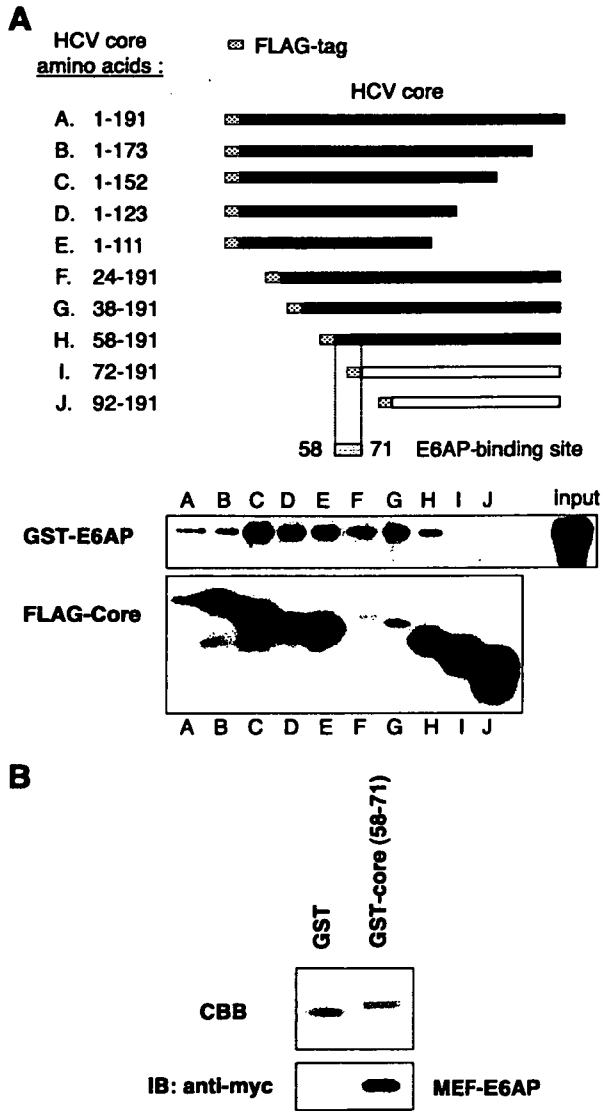

FIG. 3. Mapping of the E6AP binding domain for HCV core protein. (A) In vitro binding of E6AP to HCV core protein. 293T cells were transfected with each plasmid indicated in the upper panel. At 48 h posttransfection, cell lysates were mixed with purified GST-E6AP, immunoprecipitated with anti-FLAG beads, and then immunoblotted with anti-GST PAb (middle panel) or anti-FLAG MAb (bottom panel). The last lane (input) represents GST-E6AP used in this assay (middle panel). (B) Binding of GST-core (aa 58 to aa 71) to purified MEF-E6AP. GST served as a negative control for binding. Upper panel, Coomassie blue-stained SDS-PAGE of GST and GST-core (58–71). Lower panel, results of the GST pull-down assay. MEF-E6AP was detected by anti-myc MAb. CBB, Coomassie brilliant blue; IB, immunoblot.

duplex reduced the protein level of E6AP by 90% at 48 h posttransfection (Fig. 4C, middle panel). Immunoblotting revealed a 4.1-fold increase in the level of the core protein in the cells transfected with E6AP siRNA (Fig. 4C, top panel), suggesting that endogenous E6AP plays a role in the proteolysis of the HCV core protein.

Then we examined whether E6AP reduces the steady-state

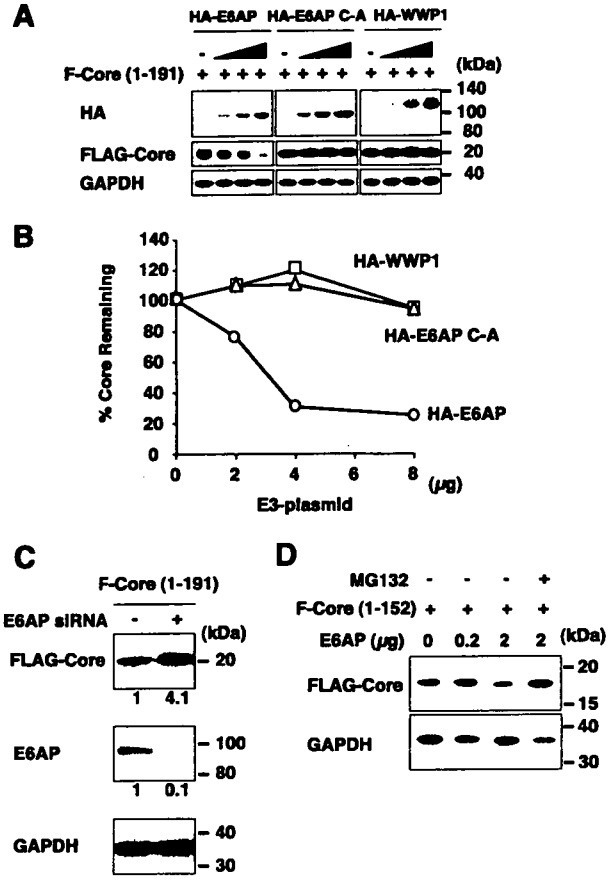

FIG. 4. E6AP decreases steady-state levels of HCV core protein in 293T cells and in HepG2 cells. (A) 293T cells (1×10^6 cells/10-cm dish) were transfected with 1 μg of pCAG FLAG-core (1–191) along with either pCAG-HA-E6AP, pCAG-HA-E6AP C-A, or pCAG-HA-WWP1 as indicated. At 48 h posttransfection, protein extracts were separated by SDS-PAGE and analyzed by immunoblotting with anti-HA PAb (top panel), anti-FLAG MAb (middle panel), and anti-GAPDH MAb (bottom panel). (B) Quantitation of data shown in panel A. Intensities of the gel bands were quantitated using the NIH Image 1.62 program. The level of GAPDH served as a loading control. Circles, E6AP; triangles, E6AP C-A; squares, WWP1. (C) Knockdown of endogenous E6AP by siRNA inhibits degradation of HCV core protein in 293T cells. 293T cells (3×10^5 cells/six-well plate) were transfected with 40 pmol of E6AP-specific duplex siRNA (or control siRNA) as described in Materials and Methods. The cells were transfected with 2 μg of FLAG-core (1–191) expression plasmid and cultured for 24 h, harvested, and analyzed by immunoblotting. Shown is immunoblot detection of FLAG-tagged core protein (top panel), E6AP protein (middle panel), and GAPDH (bottom panel) in control siRNA-treated 293T cells or E6AP-siRNA-treated 293T cells. The relative levels of protein expression were quantitated by densitometry and indicated below in the respective lanes. GAPDH served as a loading control. (D) HepG2 cells (2×10^5 cells/six-well plate) were transfected with pCAG FLAG-core (1–152) along with either empty vector or pCMV E6AP as indicated. The cells were harvested at 44 h posttransfection. Where indicated, cells were treated with 25 μM MG132 or with dimethyl sulfoxide control 14 h prior to collection. Equivalent amounts of the whole-cell lysates were separated by SDS-PAGE and analyzed by immunoblotting with anti-FLAG MAb (upper panel) or anti-GAPDH MAb (lower panel).

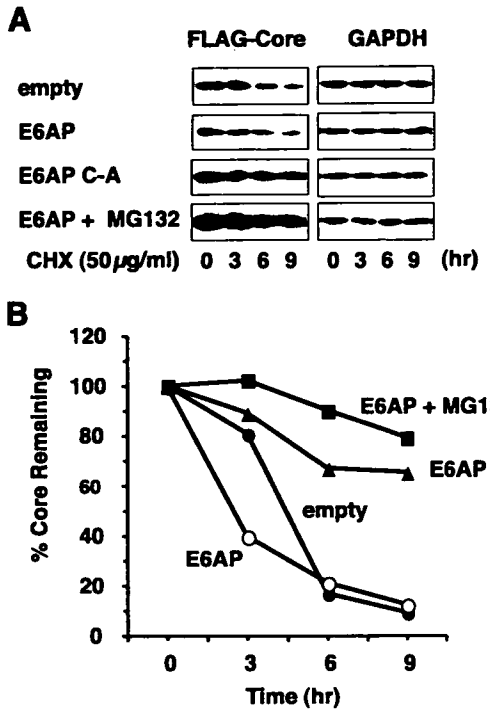

FIG. 5. Kinetic analysis of E6AP-dependent degradation of HCV core protein. (A) 293T cells (1×10^6 cells/10-cm dish) were transfected with 1 μg of pCAG-FLAG core (1–152) plus 4 μg of empty vector, pCMV-HA-E6AP, or pCMV-HA-E6AP C-A. The cells were treated with 50 μg/ml CHX at 44 h after transfection. Cell extracts were collected at 0, 3, 6, and 9 h after treatment with CHX, followed by immunoblotting. (B) Specific signals were quantitated by densitometry, and the percent remaining core at each time was compared with that at the starting point. The level of GAPDH served as a loading control. Open circles, E6AP; closed circles, empty plasmid; closed triangles, E6AP C-A; closed squares, E6AP with MG132 treatment. Data are representative of three independent experimental determinations.

levels of the core protein in hepatic cells as well as in 293T cells. Exogenous expression of E6AP resulted in reduction of the core protein in human hepatoblastoma HepG2 cells (Fig. 4D). Treatment of the cells with the proteasome inhibitor MG132 increased the core protein level, suggesting that the core protein was degraded through the ubiquitin-proteasome pathway. These results indicate that E6AP enhances proteasomal degradation of the HCV core protein in both hepatic cells and nonhepatic cells.

Kinetic analysis of E6AP-dependent degradation of HCV core protein. To determine whether the E6AP-induced reduction of the core protein is due to an increase in the rate of core degradation, we performed kinetic analysis using the protein synthesis inhibitor CHX. HCV core protein together with wild-type E6AP or inactive mutant E6AP C-A was expressed in 293T cells. At 44 h after transfection, cells were treated with either 50 μg/ml CHX alone or 50 μg/ml CHX plus 25 μM MG132 to inhibit proteasome function. Cells were collected at 0, 3, 6, and 9 h following treatment and analyzed by immunoblotting (Fig. 5A). Overexpression of E6AP resulted in rapid degradation of the core protein, whereas inactive mutant

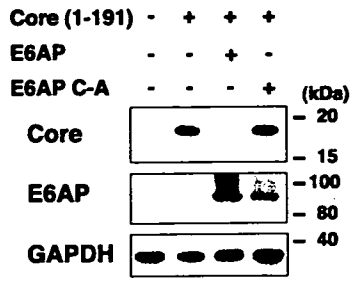

FIG. 6. E6AP promotes degradation of full-length HCV core protein in Huh-7 cells. Huh-7 cells (2×10^5 cells/six-well plate) were transfected with 0.5 μg of pCAG-core (1–191) together with 2 μg of pCMV-HA-E6AP or pCMV-HA-E6AP C-A. At 48 h posttransfection, cells were harvested and analyzed by immunoblotting with anticore MAb (top panel), anti-E6AP PAb (middle panel), or anti-GAPDH MAb (bottom panel).

E6AP C-A increased the half-life of the core protein (Fig. 5B), suggesting that the inactive E6AP inhibited degradation of the core protein in a dominant-negative manner, which is in agreement with previous studies (19, 55). Treatment of the cells with MG132 inhibited the degradation of the core protein (Fig. 5B). Reverse transcription-PCR to determine mRNA levels of the HCV core gene and GAPDH gene found that neither wild-type E6AP nor inactive E6AP changed mRNA levels of the HCV core gene and GAPDH gene (data not shown). These results indicate that E6AP enhances proteasomal degradation of the core protein.

E6AP promotes degradation of the full-length core protein in Huh-7 cells. To determine whether the full-length HCV core protein expressed in hepatic cells is degraded through an E6AP-dependent pathway, human hepatoma Huh-7 cells were transfected with pCAG HCV core (1–191) along with either E6AP or E6AP C-A. To rule out the effects of N-terminal FLAG tag on the core degradation, HCV core protein was expressed as untagged protein. Expression of wild-type E6AP resulted in reduction of the core protein (Fig. 6). On the other hand, HCV core protein was not decreased after transfection of inactive E6AP, indicating that the full-length core protein expressed in Huh-7 cells is also degraded through an E6AP-dependent pathway.

E6AP mediates ubiquitylation of HCV core protein in vivo. To determine whether E6AP can induce ubiquitylation of HCV core protein in cells, we performed in vivo ubiquitylation assays. 293T cells were cotransfected with FLAG-core (1–191) and either E6AP or empty plasmid, together with a plasmid encoding HA-tagged ubiquitin to facilitate detection of ubiquitylated core protein. Cell lysates were immunoprecipitated with anti-FLAG MAb and immunoblotted with anti-HA PAb to detect ubiquitylated core protein (Fig. 7A). Only a little ubiquitin signal was observed on the core protein in the absence of cotransfected E6AP (Fig. 7A, lane 3). In contrast, coexpression of E6AP led to readily detectable ubiquitylated forms of the core protein as a ladder and a smear of higher-molecular-weight bands (Fig. 7A, compare lane 3 with lane 4). Immunoblot analysis with anticore PAb confirmed that FLAG-core proteins were immunoprecipitated (Fig. 7B, lanes 2 to 4, short exposure) and that higher-molecular-weight bands con-